






## Syntheses, molecular structures, and self-assemblies of $SFe_3$ , $S_2Fe_3$ , $S_3Fe_5$ , $SeFe_3$ , and $Se_2Fe_3$ clusters with chelating diaminocarbenes

Yao-Cheng Shi, Shuai Wang & Sun Xie

To cite this article: Yao-Cheng Shi, Shuai Wang & Sun Xie (2015) Syntheses, molecular structures, and self-assemblies of  $SFe_3$ ,  $S_2Fe_3$ ,  $S_3Fe_5$ ,  $SeFe_3$ , and  $Se_2Fe_3$  clusters with chelating diaminocarbenes, Journal of Coordination Chemistry, 68:21, 3852-3883, DOI: [10.1080/00958972.2015.1079312](https://doi.org/10.1080/00958972.2015.1079312)


To link to this article: <http://dx.doi.org/10.1080/00958972.2015.1079312>

 View supplementary material 

 Accepted author version posted online: 10 Aug 2015.  
Published online: 23 Sep 2015.

 Submit your article to this journal 

 Article views: 37

 View related articles 

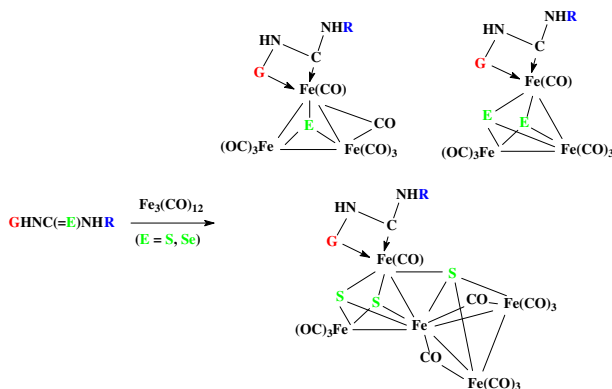
 View Crossmark data 

## Syntheses, molecular structures, and self-assemblies of $SFe_3$ , $S_2Fe_3$ , $S_3Fe_5$ , $SeFe_3$ , and $Se_2Fe_3$ clusters with chelating diaminocarbenes

YAO-CHENG SHI\*, SHUAI WANG and SUN XIE

College of Chemistry and Chemical Engineering, Yangzhou University, Yangzhou, PR China

(Received 24 March 2015; accepted 10 July 2015)



The reactions of substituted thioureas and selenoureas with iron carbonyls have been systematically investigated, and five types of  $SFe_3$ ,  $S_2Fe_3$ ,  $S_3Fe_5$ ,  $SeFe_3$ , and  $Se_2Fe_3$  clusters with chelating diaminocarbenes have been synthesized and characterized by X-ray crystallography. The reactions of  $C_3H_5NHC(=S)NHR$  with  $Fe_3(CO)_{12}$  afford  $(\mu_3-S)Fe_3(CO)_7(\mu-CO)(\kappa^3C,C,C-C_3H_5NHCNHR)$  (**1**, Ar = Ph; **2**, Ar = 4- $H_2NC_6H_4$ ). In contrast, the reactions of  $(2-C_5H_4N)NHC(=S)NHN=CHAR$  with  $Fe_2(CO)_9$  form  $(\mu_3-S)_2Fe_3(CO)_7(\kappa^2N,C-(2-C_5H_4N)NHCNHN=CHAR)$  (**3**, Ar = Ph; **4**, Ar = 4- $CH_3C_6H_4$ ). Likewise, reactions of  $GNHC(=S)NHC(=O)Ph$  with  $Fe_3(CO)_{12}$  provide  $(\mu_3-S)_2Fe_3(CO)_7(\kappa^2N,C-GNHCNHC(=O)Ph)$  (**5**, G = 2- $C_5H_4N$ ; **6**, G = 2- $C_4H_3N_2$ ) as well as  $Fe_3(CO)_8(\mu-CO)_2(\kappa^2N,C-(2-C_4H_3N_2)NHCNHC(=O)Ph)$ . The reaction of  $(2-C_5H_4N)NHC(=S)NH_2$  with  $Fe_3(CO)_{12}$  gives  $(\mu_3-S)_2Fe_3(CO)_7(\kappa^2N,C-(2-C_5H_4N)NHCNH_2)$  (**7**). The reactions of  $GNHC(=S)NHR$  with  $Fe_3(CO)_{12}$  produce  $(\mu_3-S)_2Fe_3(CO)_7(\kappa^2N,C-GNHCNHR)$  (**8**, G = 2- $C_5H_4N$ ; **9**, G = 2- $C_4H_3N_2$ ). Analogously,  $(2-C_5H_4N)NHC(=S)NH(2-CH_3C_6H_4)$  offers  $(\mu_3-S)_2Fe_3(CO)_7(\kappa^2N,C-(2-C_5H_4N)NHCNH(2-CH_3C_6H_4))$  (**10**). However,  $(2-C_5H_4N)NHC(=S)NH(2-CH_3OC_6H_4)$  generates  $(\mu_3-S)_2(\mu_4-S)Fe_5(CO)_{10}(\mu-CO)_2(\kappa^2N,C-(2-C_5H_4N)NHCNH(2-CH_3OC_6H_4))$  (**11**). Furthermore, the reactions of  $(2-C_5H_4N)NHC(=S)NHR$  with  $Fe_3(CO)_{12}$  form  $(\mu_3-S)_2(\mu_4-S)Fe_5(CO)_{10}(\mu-CO)_2(\kappa^2N,C-(2-C_5H_4N)NHCNHR)$  (**12**, R = 2- $H_2NC_6H_4$ ; **13**, R = 4- $H_2NC_6H_4$ ; **14**, R = 2- $C_5H_4N$ ). Surprisingly, the reaction of  $(2-C_5H_4N)NHC(=S)NHC_3H_5$  with  $Fe_3(CO)_{12}$  leads to  $(\mu_3-S)_2(\mu_4-S)Fe_5(CO)_{10}(\mu-CO)_2(\kappa^2N,C-(2-C_5H_4N)NHCNHC_3H_5)$  (**15**). The reaction of  $C_3H_5NHC(=Se)NHR$  with  $Fe_3(CO)_{12}$  affords  $(\mu_3-Se)Fe_3(CO)_7(\mu-CO)(\kappa^3C,C,C-C_3H_5NHCNHR)$  (**16**) as well as  $[(\kappa^2N,C-PhNCNHC_3H_5)Fe_2(CO)_6(\mu_4-Se)Fe_2(CO)_6]_2(\mu_4-Se)$ . As with  $(2-C_4H_3N_2)NHC(=S)NHR$ ,  $(2-C_4H_3N_2)NHC(=Se)$

\*Corresponding author. Email: [yeshi@yzu.edu.cn](mailto:yeshi@yzu.edu.cn)

NHPh offers  $(\mu_3\text{-Se})_2\text{Fe}_3(\text{CO})_7(\kappa^2\text{N},\text{C}\text{-}(2\text{-C}_4\text{H}_3\text{N}_2)\text{NHCNHPh})$  (**17**). Unlike  $(2\text{-C}_5\text{H}_4\text{N})\text{NHC}(=\text{S})\text{NH}(2\text{-CH}_3\text{OC}_6\text{H}_4)$ ,  $(2\text{-C}_5\text{H}_4\text{N})\text{NHC}(=\text{Se})\text{NH}(2\text{-CH}_3\text{OC}_6\text{H}_4)$  yields  $(\mu_3\text{-Se})_2\text{Fe}_3(\text{CO})_7(\kappa^2\text{N},\text{C}\text{-}(2\text{-C}_5\text{H}_4\text{N})\text{NHCNH}(2\text{-CH}_3\text{OC}_6\text{H}_4))$  (**18**). By virtue of  $\text{N}\text{-H}\cdots\text{N}$ ,  $\text{N}\text{-H}\cdots\text{O}$ , and  $\text{C}\text{-H}\cdots\text{O}$  intermolecular hydrogen bonds along with other non-covalent interactions, these new organometallic clusters exhibit interesting supramolecular structures.

*Keywords:* Fe/S cluster; Fe/Se cluster; Diaminocarbene; Thiourea; Selenourea

## 1. Introduction

Reactions of organosulfur compounds with iron carbonyls have received considerable attention because of interesting chemistry of iron–sulfur cluster complexes [1–3], and particularly because of their applications in biochemistry as models for the active sites of nitrogenases [4, 5] and [FeFe] hydrogenases [6–8]. Reactions of thiols, RSH, with iron carbonyls generally formed  $(\mu\text{-RS})_2\text{Fe}_2(\text{CO})_6$ , where the bridging thiolate acts as a three-electron donor. Moreover, butterfly complexes could be obtained by treatment of disulfides, RSSR, with iron carbonyls [9, 10]. The  $\text{Fe}_2(\text{CO})_6$  complexes might also be obtained by treating the unstable intermediates  $[\text{RSFe}(\text{CO})_4]^-$  generated from disulfides RSSR and  $\text{PPN}^+$  or  $\text{Et}_4\text{N}^+$  salts of the anion  $[\text{HFe}(\text{CO})_4]^-$  with  $\text{HBF}_4$  [11, 12]. In contrast to RSH, in refluxing THF, reactions of sodium alkanethiolates  $\text{RSNa}$  with  $\text{Fe}_3(\text{CO})_{12}$  afforded triiron anions  $[\text{Fe}_3(\text{CO})_9(\mu_3\text{-SR})]^-$ ; protonation resulted in  $\text{Fe}_3(\text{CO})_9(\mu_3\text{-SR})(\mu\text{-H})$  [13]. However, at room temperature, alkanethiolate salts, RSM ( $\text{M} = \text{Li}, \text{Na}, \text{Et}_3\text{NH}, \text{MgX}$ ), reacted with  $\text{Fe}_3(\text{CO})_{12}$  to offer salts of Seyferth-type anions  $[(\mu\text{-RS})(\mu\text{-CO})\text{Fe}_2(\text{CO})_6]^-$  [14]. Their chemistry has been extensively explored by Seyferth and Song [1, 14]. Reactions of vinylsulfides  $\text{RSCH}=\text{CH}_2$  with  $\text{Fe}_3(\text{CO})_{12}$  in refluxing benzene yielded  $(\mu\text{-RS})(\mu\text{-CH}=\text{CH}_2)\text{Fe}_2(\text{CO})_6$ , where cleavage of a C–S bond occurred and the three-electron ethenyl ligand is coordinated to the diiron core in a  $\sigma, \pi$  mode [15]. Similarly, in reactions of thioimides,  $\text{R}'\text{C}(\text{SR})=\text{NPh}$  ( $\text{R} = \text{R}' = \text{alkyl, aryl}$ ), with  $\text{Fe}_3(\text{CO})_{12}$ , scission of a C–S bond gave  $(\mu\text{-RS})(\mu\text{-R}'\text{C}=\text{NPh})\text{Fe}_2(\text{CO})_6$ , where the iminoacyl group is attached to the diiron core in a  $\sigma, \pi$  manner [16]. Closely related to the hydrodesulfurization (HDS) reaction, reactions of thiophenes,  $\text{R}_2\text{C}_4\text{H}_2\text{S}$ , and benzothiophene with  $\text{Fe}_3(\text{CO})_{12}$  have been investigated by Rauchfuss and Hirotsu [17]. Thiaferroles  $(\text{R}_2\text{C}_4\text{H}_2\text{S})\text{Fe}_2(\text{CO})_6$  and benzothiaferrole ( $\text{C}_8\text{H}_6\text{S}$ )  $\text{Fe}_2(\text{CO})_6$  were obtained. Indeed, refluxing the thiaferroles in benzene led to the corresponding desulfurized ferroles. Relying on the nature of the linking groups R and R', reactions of cyclic dithioethers,  $(\text{RSR}'\text{S})$ , with  $\text{Fe}_2(\text{CO})_9$  generated complexes of  $(\mu\text{-SRS})\text{Fe}_2(\text{CO})_6$  or  $(\mu\text{-SR}'\text{S})\text{Fe}_2(\text{CO})_6$  [18]. Analogously, cyclic dithioacetals  $\text{CH}_2(\text{SR})(\text{SR}')$  reacted with  $\text{Fe}(\text{CO})_5$  under UV irradiation to afford  $(\mu\text{-}\kappa^2\text{S},\text{C}\text{-RSCH}_2)\text{Fe}_2(\text{CO})_6(\mu\text{-SR}')$  as well as  $(\mu\text{-SCH}_2\text{S})\text{Fe}_2(\text{CO})_6$  [19]. Reactions of diaryl thioketones,  $\text{ArC}(=\text{S})\text{Ar}$ , with  $\text{Fe}_2(\text{CO})_9$  or  $\text{Fe}_3(\text{CO})_{12}$  have been studied by Alper and later by Weigand [20]. Complexes  $(\mu\text{-}\kappa^3\text{C}, \pi\text{-}(\text{Ar}'\text{CH}(\text{Ar})\text{S}))\text{Fe}_2(\text{CO})_6$  were obtained, where the  $\text{Ar}'$  group is an *ortho*-metalated Ar group and linked to the diiron core in a  $\sigma, \pi$  mode. Conversely, two types of  $\text{Fe}_2(\text{CO})_6$  complexes have been isolated from the reactions of thioesters  $\text{ArC}(=\text{S})\text{OR}$  with  $\text{Fe}_2(\text{CO})_9$ :  $(\mu\text{-}\kappa^2\text{C}, \text{O}:\kappa^2\text{S}\text{-}(\text{ArCSOR}))\text{Fe}_2(\text{CO})_6$  and  $(\mu\text{-}\kappa^3\text{C}, \pi:\kappa^2\text{S}\text{-}(\text{Ar}'\text{CH}(\text{OR})\text{S}))\text{Fe}_2(\text{CO})_6$ , where the  $\text{Ar}'$  group is an *ortho*-metalated Ar group and bonded to the diiron core in a  $\sigma, \pi$  fashion [21]. Reactions of thioamides  $\text{RC}(=\text{S})\text{NMe}_2$  ( $\text{R} = \text{Me}, \text{Ph}$ ) with  $\text{Fe}_2(\text{CO})_9$  gave both  $(\kappa\text{S}\text{-}(\text{RCSNMe}_2))\text{Fe}(\text{CO})_4$  and  $(\mu\text{-}\kappa^2\text{C}, \text{N}:\kappa^2\text{S}\text{-}(\text{RCSNMe}_2))\text{Fe}_2(\text{CO})_6$  [22]. Unlike the

thioesters and the thioamides, reactions of  $\alpha,\beta$ -unsaturated thioamides and thioesters with  $\text{Fe}(\text{CO})_5$  or  $\text{Fe}_2(\text{CO})_9$  provided  $L\text{Fe}(\text{CO})_3$ , with  $L$  as a four-electron donor being bonded via a C=C bond and an S in a  $\pi,n$  mode [23]. Reactions of dithioesters  $\text{RC}(=\text{S})\text{SR}'$  with  $\text{Fe}_2(\text{CO})_9$  produced  $(\mu-\kappa^2\text{C},\text{S}(\text{R}'):\kappa^2\text{S}-(\text{RCSSR}'))\text{Fe}_2(\text{CO})_6$ , with the organic substrate retaining its structural integrity and bonding to the diiron centers as a six-electron donor [24]. Similarly, dithioacids  $\text{RC}(=\text{S})\text{SH}$  reacted with  $\text{Fe}_3(\text{CO})_{12}$  in the presence of  $\text{Et}_3\text{N}$  at room temperature to yield  $[\text{Et}_3\text{NH}][(\mu-\text{RCS}_2)\text{Fe}_2(\text{CO})_6]$ . Reactivity of the cluster salts toward electrophiles has been investigated by Shi [25]. Interestingly, treating dithiocarbonates  $\text{ROC}(=\text{S})\text{SR}'$  with  $\text{Fe}_2(\text{CO})_9$  offered  $(\mu-\kappa^2\text{C},\text{S}(\text{R}'):\kappa^2\text{S}-(\text{ROCSSR}'))\text{Fe}_2(\text{CO})_6$ ; further heating led to  $(\mu-\text{R}'\text{S})(\mu-\text{ROC}=\text{S})\text{Fe}_2(\text{CO})_6$ , where cleavage of a C–S bond occurred with subsequent formation of bridging, three-electron thiolate and thioacyl ligands [26]. Such a cleaving reaction has been observed in the syntheses of other thiolate-bridged  $\text{Fe}_2(\text{CO})_6$  complexes as well. Complexes  $(\mu-\text{RS})(\mu-\text{RSC}=\text{S})\text{Fe}_2(\text{CO})_6$  were formed from reactions of trithiocarbonates,  $\text{RSC}(=\text{S})\text{SR}$ , with  $\text{Fe}_2(\text{CO})_9$  [26(c), 26(e)]. Reactions of substituted thioureas bearing alkyl and/or aryl group(s) with iron carbonyls have been studied by Alper and coworkers [22, 23]. Depending on the nature of the thioureas, several products such as  $(\kappa\text{S}-L)\text{Fe}(\text{CO})_4$ ,  $(\kappa\text{S}-L)_2\text{Fe}(\text{CO})_3$ ,  $(\mu-\kappa^2\text{C},\text{N}:\kappa^2\text{S}-L)\text{Fe}_2(\text{CO})_6$ , and  $(\mu-L')_2\text{Fe}_2(\text{CO})_8$  ( $L'$  = deprotonated thiourea  $L$ ) have been isolated and identified by EA, MS, and NMR. However, so far, no results on other thioureas bearing potential donors have been reported. Particularly, compared with thioureas, organometallic chemistry of selenoureas is still in its infancy [27]. Considering these reasons and our longstanding interest in the chemistry of Fe/S and Fe/Se clusters as model compounds of hydrogenases [28], we have investigated the reactions of substituted thioureas and selenoureas with iron carbonyls. Here, we report the syntheses, molecular structures, and self-assemblies of  $\text{SFe}_3$ ,  $\text{S}_2\text{Fe}_3$ ,  $\text{S}_3\text{Fe}_5$ ,  $\text{SeFe}_3$ , and  $\text{Se}_2\text{Fe}_3$  clusters with chelating diaminocarbenes.

## 2. Experimental

### 2.1. General procedures

All reactions were carried out under  $\text{N}_2$  atmosphere with standard Schlenk techniques. All solvents employed were dried by refluxing over appropriate drying agents and stored under  $\text{N}_2$  atmosphere. THF was distilled from sodium-benzophenone; petroleum ether (60–90 °C) and  $\text{CH}_2\text{Cl}_2$  were distilled from  $\text{P}_2\text{O}_5$ .  $\text{Fe}_2(\text{CO})_9$  [29],  $\text{Fe}_3(\text{CO})_{12}$  [30],  $\text{PhCONCS}$  [31],  $2\text{-C}_5\text{H}_4\text{NNCS}$  [32],  $\text{C}_3\text{H}_5\text{NCS}$  [33],  $\text{PhNCSe}$  [34],  $2\text{-CH}_3\text{OC}_6\text{H}_4\text{NCSe}$  [34],  $\text{C}_3\text{H}_5\text{NHC}(=\text{S})\text{NPh}$  (**TU1**) [35],  $\text{C}_3\text{H}_5\text{NHC}(=\text{S})\text{NH}(4\text{-H}_2\text{NC}_6\text{H}_4)$  (**TU2**) [36],  $(2\text{-C}_5\text{H}_4\text{N})\text{NHC}(=\text{S})\text{NHN}=\text{CHPh}$  (**TU3**) [37],  $(2\text{-C}_5\text{H}_4\text{N})\text{NHC}(=\text{S})\text{NHN}=\text{CH}(4\text{-CH}_3\text{C}_6\text{H}_4)$  (**TU4**) [37],  $(2\text{-C}_5\text{H}_4\text{N})\text{NHC}(=\text{S})\text{NHC}(=\text{O})\text{Ph}$  (**TU5**) [38],  $(2\text{-C}_4\text{H}_3\text{N}_2)\text{NHC}(=\text{S})\text{NHC}(=\text{O})\text{Ph}$  (**TU6**) [39],  $(2\text{-C}_5\text{H}_4\text{N})\text{NHC}(=\text{S})\text{NH}_2$  (**TU7**) [40],  $(2\text{-C}_5\text{H}_4\text{N})\text{NHC}(=\text{S})\text{NPh}$  (**TU8**) [41],  $(2\text{-C}_4\text{H}_3\text{N}_2)\text{NHC}(=\text{S})\text{NPh}$  (**TU9**) [42],  $(2\text{-C}_5\text{H}_4\text{N})\text{NHC}(=\text{S})\text{NH}(2\text{-CH}_3\text{C}_6\text{H}_4)$  (**TU10**) [43],  $(2\text{-C}_5\text{H}_4\text{N})\text{NHC}(=\text{S})\text{NH}(2\text{-CH}_3\text{OC}_6\text{H}_4)$  (**TU11**) [43],  $(2\text{-C}_5\text{H}_4\text{N})\text{NHC}(=\text{S})\text{NH}(2\text{-H}_2\text{NC}_6\text{H}_4)$  (**TU12**) [44],  $(2\text{-C}_5\text{H}_4\text{N})\text{NHC}(=\text{S})\text{NH}(4\text{-H}_2\text{NC}_6\text{H}_4)$  (**TU13**) [44],  $(2\text{-C}_5\text{H}_4\text{N})\text{NHC}(=\text{S})\text{NH}(2\text{-C}_5\text{H}_4\text{N})$  (**TU14**) [45], and  $(2\text{-C}_5\text{H}_4\text{N})\text{NHC}(=\text{S})\text{NHC}_3\text{H}_5$  (**TU15**) [46] were prepared according to the literature procedures and were identified by comparison of their melting points and IR spectra with those of authentic samples.  $\text{C}_3\text{H}_5\text{NHC}(=\text{Se})\text{NPh}$  (**SU1**),  $(2\text{-C}_4\text{H}_3\text{N}_2)\text{NHC}(=\text{Se})\text{NPh}$  (**SU2**), and  $(2\text{-C}_5\text{H}_4\text{N})\text{NHC}(=\text{Se})\text{NH}(2\text{-CH}_3\text{OC}_6\text{H}_4)$  (**SU3**) were synthesized by an

appropriate amine and isoselenocyanate of 1:1 ratio in 20 mL of  $\text{CH}_2\text{Cl}_2$  at room temperature for 4 h (see Supplementary Data) [34, 47]. The progress of all reactions was monitored by TLC (silica gel H). NMR spectra were recorded on a Bruker Avance 600 or Mercury 400 or Vx-300 spectrometer. Chemical shifts were reported in  $\delta$  units (ppm) downfield from internal tetramethylsilane for the  $^1\text{H}$  NMR spectra and for the  $^{13}\text{C}$  NMR spectra. IR spectra were carried out on a Bruker Tensor 27 spectrometer as KBr disks from 400 to  $4000\text{ cm}^{-1}$ . Analyses for C, H, and N were performed on an Elementar Vario EL analyzer. Melting points were measured on an SGW X-4 apparatus and are uncorrected.

## 2.2. Synthesis of 1

To a solution of **TU1** (0.308 g, 1.6 mmol) in THF (15 mL) was added  $\text{Fe}_3(\text{CO})_{12}$  (0.806 g, 1.6 mmol). The mixture was stirred at room temperature for 24 h. After the solvent was removed under vacuum, the residue was subjected to TLC separation using  $\text{CH}_2\text{Cl}_2$ /petroleum ether (1:2, v/v) as eluent. From the first band,  $\text{S}_2\text{Fe}_3(\text{CO})_9$  (0.075 g) was obtained which was identified by comparison of its melting point and IR spectrum with those of an authentic sample. From the second band, **1** was obtained as a brown solid (0.131 g, 14%). Anal. Calcd for  $\text{C}_{18}\text{H}_{12}\text{Fe}_3\text{N}_2\text{O}_8\text{S}$  (%): C, 37.03; H, 2.07; N, 4.80. Found: C, 37.29; H, 2.15; N, 4.67. IR (KBr): 3345 (w), 2054 (vs), 1997 (vs), 1964 (vs), 1936 (m), 1862 (m), 1556 (m), 573 (w), 538 (w)  $\text{cm}^{-1}$ .  $^1\text{H}$  NMR (300 MHz,  $\text{CDCl}_3$ , TMS):  $\delta$  7.61 (s, 1H, NH), 7.47–7.02 (m, 5H, ArH), 5.07 (s, 1H, NH), 4.32–4.31 (m, 2H,  $\text{CH}_2$ ), 4.10–4.08 (m, 1H, CH), 3.74–2.06 (m, 2H,  $\text{CH}_2$ ).  $^{13}\text{C}$  NMR (75 MHz,  $\text{CDCl}_3$ , TMS):  $\delta$  213.7, 209.0, 150.5, 131.5, 129.9, 126.8, 51.1.

## 2.3. Synthesis of 2

A mixture of **TU2** (0.207 g, 1.0 mmol) and  $\text{Fe}_3(\text{CO})_{12}$  (0.756 g, 1.5 mmol) in THF (15 mL) was stirred at room temperature for 24 h. After the solvent was removed in vacuo, the residue was subjected to TLC separation using ethyl acetate/petroleum ether (1:1, v/v) as eluent. From the first band,  $\text{S}_2\text{Fe}_3(\text{CO})_9$  (0.057 g) was obtained. From the second band, **2** was obtained as a brown solid (0.065 g, 11%). Anal. Calcd for  $\text{C}_{18}\text{H}_{13}\text{Fe}_3\text{N}_3\text{O}_8\text{S}$  (%): C, 36.10; H, 2.19; N, 7.02. Found: C, 36.02; H, 2.18; N, 7.03. IR (KBr): 3366 (w), 2060 (vs), 2004 (vs), 1958 (vs), 1863 (m), 1551 (m), 1512 (m), 575 (w), 542 (w)  $\text{cm}^{-1}$ .  $^1\text{H}$  NMR (600 MHz,  $\text{CDCl}_3$ , TMS):  $\delta$  7.39 (s, 1H, NH), 6.78–6.62 (m, 4H, ArH), 5.95 (s, 1H, NH), 4.49–4.24 (m, 2H,  $\text{CH}_2$ ), 4.08–4.06 (m, 1H, CH), 3.84–3.81 (m, 2H,  $\text{CH}_2$ ), 1.32 (s, 2H,  $\text{NH}_2$ ).

## 2.4. Synthesis of 3

A mixture of **TU3** (0.384 g, 1.5 mmol) and  $\text{Fe}_2(\text{CO})_9$  (1.637 g, 4.5 mmol) in 15 mL of toluene was stirred at room temperature for 24 h. In the course of the reaction, the pale yellow suspension slowly changed to a deep black solution as the ligand and  $\text{Fe}_2(\text{CO})_9$  dissolved. After the reaction was complete, all volatile materials were removed in vacuo. The residue was dissolved in  $\text{CH}_2\text{Cl}_2$ , 1 g of silica gel was added and the solvent was again removed under reduced pressure. Chromatography on silica gel using petroleum ether/ $\text{CH}_2\text{Cl}_2$  (1:3, v/v) as eluent afforded a grass green band of **3** (0.212 g, 44%) and  $\text{S}_2\text{Fe}_3(\text{CO})_9$  (0.052 g) in increasing order of  $R_f$  values. Anal. Calcd for  $\text{C}_{20}\text{H}_{12}\text{Fe}_3\text{N}_4\text{O}_7\text{S}_2$

(%): C, 36.84; H, 1.86; N, 8.59. Found: C, 36.71; H, 1.83; N, 8.68. IR (KBr): 3352 (m), 2923 (m), 2852 (m), 2057 (s), 2001 (vs), 1969 (vs), 1915 (s), 1610 (w), 1525 (m), 1261 (w), 808 (m), 579 (w)  $\text{cm}^{-1}$ .  $^1\text{H}$  NMR (600 MHz,  $\text{CDCl}_3$ , TMS):  $\delta$  9.66 (s, 1H), 9.09 (s, 1H), 8.12 (s, 1H), 8.01 (s, 1H), 7.76 (s, 2H), 7.65 (s, 1H), 7.49 (s, 3H), 7.07 (s, 1H), 6.94 (s, 1H).

## 2.5. Synthesis of 4

Similar to **TU3**, **TU4** (0.405 g, 1.5 mmol) and  $\text{Fe}_2(\text{CO})_9$  (1.637 g, 4.5 mmol) gave, using petroleum ether/ $\text{CH}_2\text{Cl}_2$  (1:2, v/v) as eluent,  $\text{S}_2\text{Fe}_3(\text{CO})_9$  (0.053 g) and **4** (0.223 g, 44%). Anal. Calcd for  $\text{C}_{21}\text{H}_{14}\text{Fe}_3\text{N}_4\text{O}_7\text{S}_2$  (%): C, 37.87; H, 2.12; N, 8.41. Found: C, 37.89; H, 2.14; N, 8.39. IR (KBr): 3321 (m), 2849 (m), 2087 (vs), 2019 (vs), 1988 (s), 1599 (w), 1488 (m), 1297 (w), 1255 (w), 1088 (w), 1029 (w), 757 (m), 697 (m), 666 (w), 593 (w), 560 (w), 512 (w)  $\text{cm}^{-1}$ .  $^1\text{H}$  NMR (600 MHz,  $\text{CDCl}_3$ , TMS):  $\delta$  9.63 (s, 1H), 9.03 (s, 1H), 8.11 (s, 1H), 7.97 (s, 1H), 7.65 (s, 4H), 7.01–6.89 (d, 3H), 2.43 (s, 3H).

## 2.6. Synthesis of 5

To a solution of **TU5** (0.401 g, 1.56 mmol) in 15 mL of THF was added  $\text{Fe}_3(\text{CO})_{12}$  (0.786 g, 1.56 mmol). The mixture was stirred at room temperature for 24 h. After the solvent was removed under vacuum, the residue was subjected to TLC separation using  $\text{CH}_2\text{Cl}_2$ /petroleum ether (3:20, v/v) as eluent. From the first band,  $\text{S}_2\text{Fe}_3(\text{CO})_9$  (0.148 g) was obtained. From the second band, **5** was obtained as a brown solid (0.311 g, 60%). Anal. Calcd for  $\text{C}_{20}\text{H}_{11}\text{Fe}_3\text{N}_3\text{O}_8\text{S}_2$  (%): C, 36.79; H, 1.70; N, 6.44. Found: C, 36.83; H, 1.76; N, 6.40. IR (KBr): 3229 (w), 2058 (vs), 2014 (vs), 1686 (m), 1500 (m), 1331 (w), 772 (w)  $\text{cm}^{-1}$ .  $^1\text{H}$  NMR (500 MHz,  $\text{CDCl}_3$ , TMS):  $\delta$  13.05 (s, 1H, NH), 9.99 (s, 1H, NH), 8.21–7.08 (m, 9H, ArH).  $^{13}\text{C}$  NMR (126 MHz,  $\text{CDCl}_3$ , TMS):  $\delta$  235.9, 217.6, 211.2, 207.0, 206.9, 184.3, 165.5, 156.9, 147.6, 137.7, 134.4, 129.6, 119.3, 112.3.

## 2.7. Synthesis of 6

Similar to **TU5**, **TU6** (0.258 g, 1.0 mmol) and  $\text{Fe}_3(\text{CO})_{12}$  (0.504 g, 1.0 mmol) afforded, after TLC separation using  $\text{CH}_2\text{Cl}_2$ /petroleum ether (1:2, v/v) as eluent,  $\text{S}_2\text{Fe}_3(\text{CO})_9$  (0.083 g), **6** as a brown-black solid (0.082 g, 26%), and  $\text{C}_{22}\text{H}_{10}\text{Fe}_3\text{N}_4\text{O}_{11}$  as a green solid (0.014 g, 2%) in decreasing order of  $R_f$  values. Anal. Calcd for  $\text{C}_{22}\text{H}_{10}\text{Fe}_3\text{N}_4\text{O}_{11}$  (%): C, 39.21; H, 1.50; N, 8.31. Found: C, 39.34; H, 1.56; N, 8.32. IR (KBr): 3199 (w), 2072 (vs), 2016 (vs), 1982 (vs), 1954 (vs), 1854 (m), 1673 (m), 1524 (m), 1349 (m), 768 (w), 705 (w), 668 (w). Anal. Calcd for  $\text{C}_{19}\text{H}_{10}\text{Fe}_3\text{N}_4\text{O}_8\text{S}_2$  (%): C, 34.90; H, 1.54; N, 8.57. Found: C, 34.96; H, 1.58; N, 8.56. IR (KBr): 3219 (w), 2058 (vs), 2018 (vs), 1974 (vs), 1944 (vs), 1687 (w), 1492 (m), 1251 (w), 803 (w), 704 (w), 582 (w)  $\text{cm}^{-1}$ .  $^1\text{H}$  NMR (300 MHz,  $\text{CD}_3\text{COCD}_3$ , TMS):  $\delta$  13.26 (s, 1H, NH), 10.57 (s, 1H, NH), 8.74–7.36 (m, 8H, ArH).

## 2.8. Synthesis of 7

A mixture of **TU7** (0.306 g, 2.0 mmol) and  $\text{Fe}_3(\text{CO})_{12}$  (1.007 g, 2.0 mmol) in 15 mL THF was stirred at room temperature for 24 h. After the solvent was removed under vacuum, the residue was subjected to TLC separation using ethyl acetate/petroleum ether (1:2, v/v) as

eluent. From the first band,  $S_2Fe_3(CO)_9$  (0.080 g) was obtained. From the second band, **7** was obtained as a brown solid (0.110 g, 10%). Anal. Calcd for  $C_{13}H_7Fe_3N_3O_7S_2$  (%): C, 28.45; H, 1.29; N, 7.66. Found: C, 28.42; H, 1.31; N, 7.68. IR (KBr): 3415 (w), 3294 (w), 2921 (m), 2852 (w), 2053 (vs), 2014 (vs), 1976 (vs), 1930 (vs), 1695 (w), 1620 (w), 1481 (w), 1449 (w), 1343 (w), 767 (w), 717 (w)  $cm^{-1}$ .  $^1H$  NMR (300 MHz,  $CD_3COCD_3$ , TMS):  $\delta$  10.54 (s, 1H, NH), 8.01–6.98 (m, 4H, ArH), 2.80 (s, 2H,  $NH_2$ ).  $^{13}C$  NMR (75 MHz,  $CD_3COCD_3$ , TMS):  $\delta$  213.0, 209.2, 147.5, 139.4, 118.4, 111.1.

### 2.9. Synthesis of **8**

Similar to **TU7**, **TU8** (0.344 g, 1.5 mmol) and  $Fe_3(CO)_{12}$  (0.756 g, 1.5 mmol) afforded, using  $CH_2Cl_2$ /petroleum ether (1:4, v/v) as eluent,  $S_2Fe_3(CO)_9$  (0.099 g) and **8** as a brown solid (0.273 g, 58%). Anal. Calcd for  $C_{19}H_{11}Fe_3N_3O_7S_2$  (%): C, 36.51; H, 1.77; N, 6.72. Found: C, 36.62; H, 1.79; N, 6.75. IR (KBr): 3033 (w), 2055 (vs), 2007 (vs), 1671 (w), 1599 (m), 1532 (m), 1478 (m), 772 (w), 699 (w)  $cm^{-1}$ .  $^1H$  NMR (500 MHz,  $CD_3COCD_3$ , TMS):  $\delta$  10.37 (s, 1H, NH), 9.27 (s, 1H, NH), 8.11–7.04 (m, 9H, ArH).  $^{13}C$  NMR (126 MHz,  $CD_3COCD_3$ , TMS):  $\delta$  213.1, 209.2, 147.6, 139.4, 131.0, 129.0, 127.0, 119.0, 112.1.

### 2.10. Synthesis of **9**

Analogous to **TU8**, **TU9** (0.368 g, 1.6 mmol) and  $Fe_3(CO)_{12}$  (0.806 g, 1.6 mmol) in 15 mL of THF gave, after TLC separation using  $CH_2Cl_2$ /petroleum ether (1:1, v/v) as eluent,  $S_2Fe_3(CO)_9$  (0.089 g) and **9** as a brown solid (0.152 g, 30%). Anal. Calcd for  $C_{18}H_{10}Fe_3N_4O_7S_2$  (%): C, 34.54; H, 1.61; N, 8.95. Found: C, 34.51; H, 1.63; N, 8.97. IR (KBr): 3026 (w), 2055 (vs), 2013 (vs), 1983 (vs), 1952 (vs), 1920 (m), 1525 (m), 801 (w), 771 (w), 694 (w)  $cm^{-1}$ .  $^1H$  NMR (300 MHz,  $CD_3COCD_3$ , TMS):  $\delta$  10.47 (s, 1H, NH), 9.49 (s, 1H, NH), 8.56–7.15 (m, 8H, ArH).  $^{13}C$  NMR (75 MHz,  $CD_3COCD_3$ , TMS):  $\delta$  213.0, 206.1, 159.3, 157.3, 131.0, 129.2, 126.9, 115.3, 115.2.

### 2.11. Synthesis of **10**

Similar to **TU9**, **TU10** (0.243 g, 1.0 mmol) and  $Fe_3(CO)_{12}$  (0.504 g, 1.0 mmol) afforded, after TLC separation using  $CH_2Cl_2$ /petroleum ether (3:10, v/v) as eluent,  $S_2Fe_3(CO)_9$  (0.068 g) and **10** as a brown solid (0.064 g, 20%). Anal. Calcd for  $C_{20}H_{13}Fe_3N_3O_7S_2$  (%): C, 37.59; H, 2.05; N, 6.58. Found: C, 37.45; H, 2.08; N, 6.67. IR (KBr): 3028 (w), 2059 (vs), 2016 (vs), 1938 (s), 1909 (m), 1526 (m), 582 (m)  $cm^{-1}$ .  $^1H$  NMR (300 MHz,  $CDCl_3$ , TMS):  $\delta$  8.12–7.40 (m, 8H, ArH), 6.90 (s, 1H, NH), 6.80 (s, 1H, NH), 2.33 (s, 3H,  $CH_3$ ).  $^{13}C$  NMR (75 MHz,  $CDCl_3$ , TMS):  $\delta$  224.9, 220.0, 212.1, 207.4, 157.0, 147.8, 137.3, 132.3, 127.6, 127.0, 117.8, 109.8, 17.6.

### 2.12. Synthesis of **11**

To a solution of **TU11** (0.259 g, 1.0 mmol) in 15 mL of THF was added  $Fe_3(CO)_{12}$  (0.756 g, 1.5 mmol). The mixture was stirred at room temperature for 24 h. After the solvent was removed in vacuo, the residue was subjected to TLC separation using  $CH_2Cl_2$ /petroleum ether (1:1, v/v) as eluent. From the first band,  $S_2Fe_3(CO)_9$  (0.068 g) was

obtained. From the second band, **11** was obtained as a black solid (0.085 g, 27%). Anal. Calcd for  $C_{25}H_{13}Fe_5N_3O_{13}S_3$  (%): C, 31.98; H, 1.40; N, 4.48. Found: C, 32.05; H, 1.43; N, 4.51. IR (KBr): 3223 (w), 2059 (vs), 2013 (vs), 1906 (m), 1829 (m), 1523 (m), 581 (w)  $cm^{-1}$ .  $^1H$  NMR (300 MHz,  $CD_3COCD_3$ , TMS):  $\delta$  7.89 (s, 1H, NH), 7.55–7.04 (m, 8H, ArH), 5.62 (s, 1H, NH), 3.95 (s, 3H,  $CH_3$ ).  $^{13}C$  NMR (75 MHz,  $CD_3COCD_3$ , TMS):  $\delta$  221.4, 219.3, 146.8, 139.7, 130.2, 127.1, 118.4, 112.8, 111.9, 55.5.

### 2.13. Synthesis of **12**

A mixture of **TU12** (0.366 g, 1.5 mmol) and  $Fe_3(CO)_{12}$  (1.133 g, 2.25 mmol) in 15 mL of THF was stirred at 50 °C for 4 h. After removal of the solvent under vacuum, the residue was subjected to TLC separation using  $CH_2Cl_2$  as eluent. From the first band,  $S_2Fe_3(CO)_9$  (0.055 g) was obtained. From the second band, **12** was obtained as a brown solid (0.108 g, 24%). Anal. Calcd for  $C_{24}H_{12}Fe_5N_4O_{12}S_3$  (%): C, 31.20; H, 1.31; N, 6.06. Found: C, 31.23; H, 1.34; N, 6.02. IR (KBr): 3336 (w), 2070 (m), 2045 (vs), 2023 (vs), 1986 (vs), 1820 (m), 1615 (w), 1525 (w), 1483 (w), 775 (w), 607 (w), 572 (w)  $cm^{-1}$ .  $^1H$  NMR (600 MHz,  $CDCl_3$ , TMS):  $\delta$  8.56 (s, 1H, NH), 7.72 (s, 1H, NH), 7.57–6.90 (m, 8H, ArH), 4.06 (s, 2H,  $NH_2$ ).

### 2.14. Synthesis of **13**

Similar to **TU12**, **TU13** (0.366 g, 1.5 mmol) and  $Fe_3(CO)_{12}$  (1.133 g, 2.25 mmol) afforded, using  $CH_2Cl_2$  as eluent,  $S_2Fe_3(CO)_9$  (0.049 g) and **13** as a brown solid (0.097 g, 21%). Anal. Calcd for  $C_{24}H_{12}Fe_5N_4O_{12}S_3$  (%): C, 31.20; H, 1.31; N, 6.06. Found: C, 31.25; H, 1.28; N, 6.08. IR (KBr): 3347 (w), 2069 (m), 2042 (vs), 2019 (vs), 1982 (vs), 1830 (m), 1529 (m), 607 (m)  $cm^{-1}$ .  $^1H$  NMR (600 MHz,  $CDCl_3$ , TMS):  $\delta$  8.68 (s, 1H, NH), 7.90–6.78 (m, 8H, ArH), 4.48 (s, 1H, NH), 2.72 (s, 2H,  $NH_2$ ).

### 2.15. Synthesis of **14**

Analogous to **TU11**, **TU14** (0.230 g, 1.0 mmol) and  $Fe_3(CO)_{12}$  (0.756 g, 1.5 mmol) gave, after TLC separation using  $CH_2Cl_2$ /petroleum ether (1:3, v/v) as eluent,  $S_2Fe_3(CO)_9$  (0.051 g) and **14** as a brown solid (0.082 g, 27%). Anal. Calcd for  $C_{23}H_{10}Fe_5N_4O_{12}S_3$  (%): C, 30.36; H, 1.11; N, 6.16. Found: C, 30.42; H, 1.17; N, 6.22. IR (KBr): 3344 (w), 2917 (w), 2047 (vs), 2015 (vs), 1926 (m), 1832 (m), 1599 (m), 1516 (m), 1475 (m), 774 (w), 606 (w), 570 (w)  $cm^{-1}$ .  $^1H$  NMR (600 MHz,  $CD_3COCD_3$ , TMS):  $\delta$  14.48 (s, 1H, NH), 9.53 (s, 1H, NH), 8.42–7.15 (m, 8H, ArH).

### 2.16. Synthesis of **15**

Similar to **TU14**, **TU15** (0.309 g, 1.6 mmol) and  $Fe_3(CO)_{12}$  (1.209 g, 2.4 mmol) afforded, after TLC separation using  $CH_2Cl_2$ /petroleum ether (2:1, v/v) as eluent,  $S_2Fe_3(CO)_9$  (0.045 g) and **15** as a brown solid (0.112 g, 24%). Anal. Calcd for  $C_{21}H_{11}Fe_5N_3O_{12}S_3$  (%): C, 28.90; H, 1.27; N, 4.81. Found: C, 28.94; H, 1.31; N, 4.82. IR (KBr): 3362 (w), 2047 (vs), 1989 (vs), 1839 (m), 1553 (w), 1485 (w), 606 (w), 572 (w)  $cm^{-1}$ .  $^1H$  NMR (600 MHz,  $CDCl_3$ , TMS):  $\delta$  10.44 (s, 1H, NH), 8.04 (s, 1H, NH), 7.76–7.03 (m, 4H, ArH),



5.99–5.90 (m, 1H, CH), 5.30–5.22 (m, 2H, CH<sub>2</sub>), 4.25–4.23 (m, 2H, CH<sub>2</sub>). <sup>13</sup>C NMR (151 MHz, CDCl<sub>3</sub>, TMS): δ 213.0, 147.5, 139.5, 133.6, 118.7, 116.2, 111.5, 55.2, 46.7.

### 2.17. Synthesis of 16

Solution of **SU1** (0.239 g, 1.0 mmol) in 15 mL of THF was cooled to 0 °C, then Fe<sub>3</sub>(CO)<sub>12</sub> (0.756 g, 1.5 mmol) was added. The resulting mixture was stirred in the dark at room temperature for 24 h. After the solvent was removed in vacuo, the residue was subjected to TLC separation using CH<sub>2</sub>Cl<sub>2</sub>/petroleum ether (1:5, v/v) as eluent. From the first band was obtained Se<sub>2</sub>Fe<sub>3</sub>(CO)<sub>9</sub> (0.043 g) which was identified by comparison of its melting point and IR spectrum with those of an authentic sample. From the second band, C<sub>44</sub>H<sub>22</sub>Fe<sub>8</sub>N<sub>4</sub>O<sub>24</sub>Se<sub>3</sub> was obtained as a brown solid (0.084 g, 10%). When the eluent was changed to CH<sub>2</sub>Cl<sub>2</sub>/petroleum ether (1:2, v/v), **16** was obtained as a black solid (0.019 g, 3%). Anal. Calcd for C<sub>44</sub>H<sub>22</sub>Fe<sub>8</sub>N<sub>4</sub>O<sub>24</sub>Se<sub>3</sub> (%): C, 31.56; H, 1.32; N, 3.35. Found: C, 31.59; H, 1.37; N, 3.38. IR (KBr): 3321 (w), 2910 (w), 2051 (vs), 1988 (vs), 1523 (w), 610 (w) cm<sup>-1</sup>. <sup>1</sup>H NMR (300 MHz, CD<sub>3</sub>COCD<sub>3</sub>, TMS): δ 7.43–7.00 (m, 10H, ArH), 5.91–5.80 (m, 2H, 2CH), 5.18–5.16 (m, 4H, 2CH<sub>2</sub>), 3.95 (s, br, 2H, 2NH), 2.97–2.61 (m, 4H, 2CH<sub>2</sub>). Anal. Calcd for C<sub>18</sub>H<sub>12</sub>Fe<sub>3</sub>N<sub>2</sub>O<sub>8</sub>Se (%): C, 34.27; H, 1.92; N, 4.44. Found: C, 34.19; H, 1.88; N, 4.41. IR (KBr): 3328 (w), 2862 (w), 2052 (s), 1999 (vs), 1955 (vs), 1956 (vs), 1856 (m), 1548 (m), 575 (w), 535 (w) cm<sup>-1</sup>. <sup>1</sup>H NMR (400 MHz, CD<sub>3</sub>COCD<sub>3</sub>, TMS): δ 7.59 (s, 1H, NH), 7.46–7.00 (m, 5H, ArH), 5.12 (s, 1H, NH), 4.31–4.28 (m, 2H, CH<sub>2</sub>), 4.11–4.07 (m, 1H, CH), 3.62–2.05 (m, 2H, CH<sub>2</sub>). <sup>13</sup>C NMR (100 MHz, CD<sub>3</sub>COCD<sub>3</sub>, TMS): δ 213.4, 209.3, 152.1, 131.4, 128.3, 126.2, 114.8, 44.2.

### 2.18. Synthesis of 17

Similar to **SU1**, **SU2** (0.277 g, 1.0 mmol) and Fe<sub>3</sub>(CO)<sub>12</sub> (0.504 g, 1.0 mmol) provided, after TLC separation using CH<sub>2</sub>Cl<sub>2</sub>/petroleum ether (2:3, v/v) as eluent, Se<sub>2</sub>Fe<sub>3</sub>(CO)<sub>9</sub> (0.046 g) and **17** as a brown solid (0.085 g, 24%). Anal. Calcd for C<sub>18</sub>H<sub>10</sub>Fe<sub>3</sub>N<sub>4</sub>O<sub>7</sub>Se<sub>2</sub> (%): C, 30.04; H, 1.40; N, 7.78. Found: C, 30.11; H, 1.43; N, 7.69. IR (KBr): 3331 (w), 2051 (vs), 2013 (vs), 1966 (vs), 1919 (vs), 1588 (w), 1520 (m), 1366 (w), 802 (w), 671 (w), 607 (w) cm<sup>-1</sup>. <sup>1</sup>H NMR (300 MHz, CD<sub>3</sub>COCD<sub>3</sub>, TMS): δ 10.46 (s, 1H, NH), 9.56 (s, 1H, NH), 8.56–7.40 (m, 8H, ArH). <sup>13</sup>C NMR (75 MHz, CD<sub>3</sub>COCD<sub>3</sub>, TMS): δ 214.5, 210.5, 159.2, 157.6, 131.0, 129.2, 126.9, 116.3.

### 2.19. Synthesis of 18

Analogous to **SU2**, **SU3** (0.306 g, 1.0 mmol) and Fe<sub>3</sub>(CO)<sub>12</sub> (0.504 g, 1.0 mmol) afforded, after TLC separation using CH<sub>2</sub>Cl<sub>2</sub>/petroleum ether (1:1, v/v) as eluent, Se<sub>2</sub>Fe<sub>3</sub>(CO)<sub>9</sub> (0.055 g) and **18** as a brown solid (0.152 g, 40%). Anal. Calcd for C<sub>20</sub>H<sub>13</sub>Fe<sub>3</sub>N<sub>3</sub>O<sub>8</sub>Se<sub>2</sub> (%): C, 32.08; H, 1.75; N, 5.61. Found: C, 32.16; H, 1.82; N, 5.49. IR (KBr): 3363 (w), 2838 (w), 2045 (vs), 2003 (vs), 1957 (vs), 1926 (vs), 1521 (vs), 1261 (w), 1151 (w), 759 (w), 604 (w), 585 (w) cm<sup>-1</sup>. <sup>1</sup>H NMR (300 MHz, CD<sub>3</sub>COCD<sub>3</sub>, TMS): δ 8.98 (s, 1H, NH), 8.37 (s, 1H, NH), 8.11–7.03 (m, 8H, ArH), 3.90 (s, 3H, CH<sub>3</sub>). <sup>13</sup>C NMR (75 MHz, CD<sub>3</sub>COCD<sub>3</sub>, TMS): δ 213.6, 209.7, 146.9, 138.3, 129.7, 127.6, 117.9, 112.7, 110.9, 55.4.

## 2.20. X-ray determinations of 1–18

Single crystals of  $C_{22}H_{10}Fe_3N_4O_{11}$ ,  $C_{44}H_{22}Fe_8N_4O_{24}Se_3$ , and **1–18** suitable for X-ray diffraction analyses were grown by slow evaporation of the  $CH_2Cl_2$ -petroleum ether solutions at 0–4 °C. For each cluster, a selected single crystal was mounted on a Bruker APEX II CCD diffractometer which used graphite-monochromated Mo-K $\alpha$  radiation ( $\lambda = 0.71073$  Å) at 296 K. The structures were solved by direct methods using SIR-2011 [48] and refined by full-matrix least-squares based on  $F^2$  with anisotropic thermal parameters for all non-hydrogen atoms using SHELXTL [49] and WinGX [50]. Anisotropic displacement parameters were refined for all non-hydrogen atoms. All N-bound H atoms were determined from Fourier difference maps and refined independently in isotropic approximation except for **12** and **13**, whereas all C-bound H atoms were placed at geometrically idealized positions and subsequently treated as riding with C–H = 0.93 (aromatic, olefinic), 0.98 (CH), 0.97 (CH<sub>2</sub>), 0.96 (CH<sub>3</sub>) Å and  $U_{iso}(H)$  values of 1.2  $U_{eq}(C, N)$  and 1.5  $U_{eq}(CH_3)$ . All interactions and close contacts were analyzed with PLATON [51] and MERCURY [52]. For **5**, poor data does not afford accurate geometric parameters (crystal data for **5**:  $C_{20}H_{11}Fe_3N_3O_8S_2$ , Fw = 652.99, monoclinic, space group  $P 2_1/c$ ,  $a = 16.8042(12)$ ,  $b = 12.757(2)$ ,  $c = 24.3897(12)$ ,  $\beta = 96.7997(15)^\circ$ ,

Table 1. Crystal data and structure refinements for **1–4** and **6**.

	<b>1</b>	<b>2</b>	<b>3</b>	<b>4</b>	<b>6</b>
Formula	$C_{18}H_{12}Fe_3N_2O_8S$	$C_{18}H_{13}Fe_3N_3O_8S$	$C_{20}H_{12}Fe_3N_4O_7S_2$	$C_{21}H_{14}Fe_3N_4O_7S_2$	$C_{19}H_{10}Fe_3N_4O_8S_2$
Fw	583.91	598.92	652.01	666.03	653.98
Cryst system	Monoclinic	Triclinic	Monoclinic	Monoclinic	Triclinic
Space group	$P 2_1/c$	$P \bar{1}$	$P 2_1/c$	$I 2/a$	$P \bar{1}$
$a$ (Å)	10.0221(9)	8.2495(18)	25.552(3)	17.4507(19)	9.7877(19)
$b$ (Å)	18.0078(16)	9.675(2)	11.4537(15)	11.5081(16)	10.1430(11)
$c$ (Å)	14.9644(2)	14.7681(13)	17.622(2)	26.531(2)	13.3690(13)
$\alpha$ (°)	90.00	84.226(2)	90.00	90.00	91.463(2)
$\beta$ (°)	126.989(4)	74.857(3)	104.655(2)	100.835(3)	106.746(3)
$\gamma$ (°)	90.00	84.899(3)	90.00	90.00	108.144(2)
$V$ (Å <sup>3</sup> )	2157.2(3)	1129.6(4)	4989.6(10)	5233.1(10)	1198.0(3)
$Z$	4	2	8	8	2
$D_c$ (g/cm <sup>-3</sup> )	1.798	1.761	1.736	1.691	1.813
$\mu$ /mm <sup>-1</sup>	2.135	2.042	1.936	1.848	2.020
$F(0\ 0\ 0)$	1168	600	2608	2672	652
Index ranges	$-12 \leq h \leq 12$ $-23 \leq k \leq 23$ $-18 \leq l \leq 19$	$-10 \leq h \leq 10$ $-12 \leq k \leq 12$ $-19 \leq l \leq 19$	$-33 \leq h \leq 32$ $-14 \leq k \leq 14$ $-22 \leq l \leq 22$	$-22 \leq h \leq 22$ $-13 \leq k \leq 14$ $-34 \leq l \leq 34$	$-11 \leq h \leq 12$ $-13 \leq k \leq 12$ $-17 \leq l \leq 17$
Measured data	18,486	9923	42,675	21,996	10,637
Unique data	4921	5066	11,335	6078	5400
Data [ $I > 2\sigma(I)$ ]	4167	2329	6341	4233	2916
$R_{int}$	0.053	0.060	0.085	0.065	0.051
$\theta_{max}$ (°)	27.5	27.5	27.5	27.7	27.6
Refined parameters	297	304	664	335	331
$R_1$	0.0313	0.0507	0.0474	0.0541	0.0453
$wR_2$	0.0816	0.1235	0.1195	0.1652	0.0949
GOF	1.07	0.91	0.98	1.06	0.92
Peak/hole	0.36/–0.67	0.50/–0.36	0.71/–0.45	1.07/–1.13	0.39/–0.37

Table 2. Crystal data and structure refinements for 7–12.

	7	8-CH <sub>2</sub> Cl <sub>2</sub>	9	10	11-0.5CH <sub>2</sub> Cl <sub>2</sub>	12
Formula	C <sub>13</sub> H <sub>2</sub> Fe <sub>3</sub> N <sub>3</sub> O <sub>7</sub> S <sub>2</sub>	C <sub>20</sub> H <sub>13</sub> Cl <sub>2</sub> Fe <sub>3</sub> N <sub>3</sub> O <sub>7</sub> S <sub>2</sub>	C <sub>18</sub> H <sub>10</sub> Fe <sub>3</sub> N <sub>4</sub> O <sub>7</sub> S <sub>2</sub>	C <sub>20</sub> H <sub>13</sub> Fe <sub>3</sub> N <sub>3</sub> O <sub>7</sub> S <sub>2</sub>	C <sub>51</sub> H <sub>28</sub> Cl <sub>2</sub> Fe <sub>10</sub> N <sub>6</sub> O <sub>18</sub> S <sub>6</sub>	C <sub>24</sub> H <sub>12</sub> Fe <sub>3</sub> N <sub>4</sub> O <sub>12</sub> S <sub>3</sub>
Fw	548.89	709.90	625.97	639.00	1962.55	923.81
Cryst system	Monoclinic	Tritrilinec	Monoclinic	Orthorhombic	Monoclinic	Monoclinic
Space group	<i>P</i> 2 <sub>1</sub> / <i>c</i>	<i>P</i> 1	<i>P</i> 2 <sub>1</sub> / <i>c</i>	<i>P</i> <i>ccn</i>	<i>P</i> 2 <sub>1</sub> / <i>c</i>	<i>P</i> 2 <sub>1</sub> / <i>c</i>
<i>a</i> (Å)	11.0235(14)	9.7729(13)	9.4660(13)	15.615(3)	10.7344(14)	9.9261(14)
<i>b</i> (Å)	15.4097(16)	11.4397(15)	17.884(2)	27.199(3)	19.169(3)	19.8343(11)
<i>c</i> (Å)	13.0895(12)	12.5392(17)	13.9509(19)	11.561(4)	18.297(2)	16.7076(16)
<i>α</i> (°)	90.00	85.5268(14)	90.00	90.00	90.00	90.00
<i>β</i> (°)	122.360(4)	82.5564(15)	102.960(2)	90.00	98.079(2)	92.965(2)
<i>γ</i> (°)	90.00	79.2132(16)	90.00	90.00	90.00	90.00
<i>V</i> [Å <sup>3</sup> ]	1878.2(4)	1363.4(3)	2301.6(5)	4910(2)	3727.6(9)	3284.9(6)
<i>Z</i>	4	2	4	8	2	4
<i>D</i> <sub>c</sub> [g/cm <sup>-3</sup> ]	1.941	1.729	1.806	1.729	1.748	1.868
<i>μ</i> [mm <sup>-1</sup> ]	2.550	1.968	2.095	1.965	2.201	2.411
<i>F</i> (0 0 0)	1088	708	1248	2560	1948	1832
Index ranges	-14 ≤ <i>h</i> ≤ 14 -19 ≤ <i>k</i> ≤ 20 -17 ≤ <i>l</i> ≤ 17	-12 ≤ <i>h</i> ≤ 12 -14 ≤ <i>k</i> ≤ 14 -16 ≤ <i>l</i> ≤ 16	-12 ≤ <i>h</i> ≤ 12 -23 ≤ <i>k</i> ≤ 23 -18 ≤ <i>l</i> ≤ 17	-17 ≤ <i>h</i> ≤ 20 -35 ≤ <i>k</i> ≤ 35 -14 ≤ <i>l</i> ≤ 14	-13 ≤ <i>h</i> ≤ 13 -24 ≤ <i>k</i> ≤ 24 -23 ≤ <i>l</i> ≤ 23	-12 ≤ <i>h</i> ≤ 12 -24 ≤ <i>k</i> ≤ 25 -21 ≤ <i>l</i> ≤ 21
Measured data	16,318	11,764	19,837	40,918	32,020	28,120
Unique data	4331	6106	5242	5638	8503	7479
Data [ <i>I</i> > 2σ( <i>I</i> )]	3306	5160	3945	3350	4852	3204
<i>R</i> <sub>int</sub>	0.061	0.039	0.051	0.096	0.056	0.143
<i>θ</i> <sub>max</sub> (°)	27.6	27.5	27.5	27.5	27.5	27.5
Refined parameters	265	364	315	325	529	439
<i>R</i> <sub>1</sub>	0.0343	0.0392	0.0338	0.0443	0.0516	0.0751
w <i>R</i> <sub>2</sub>	0.0833	0.1152	0.0860	0.0926	0.1766	0.1894
GOF	1.02	1.05	1.07	1.01	1.02	0.98
Peak/hole	0.34/-0.41	0.78/-0.48	0.35/-0.37	0.41/-0.29	0.93/-0.48	0.81/-0.72

Table 3. Crystal data and structure refinements for 13–18.

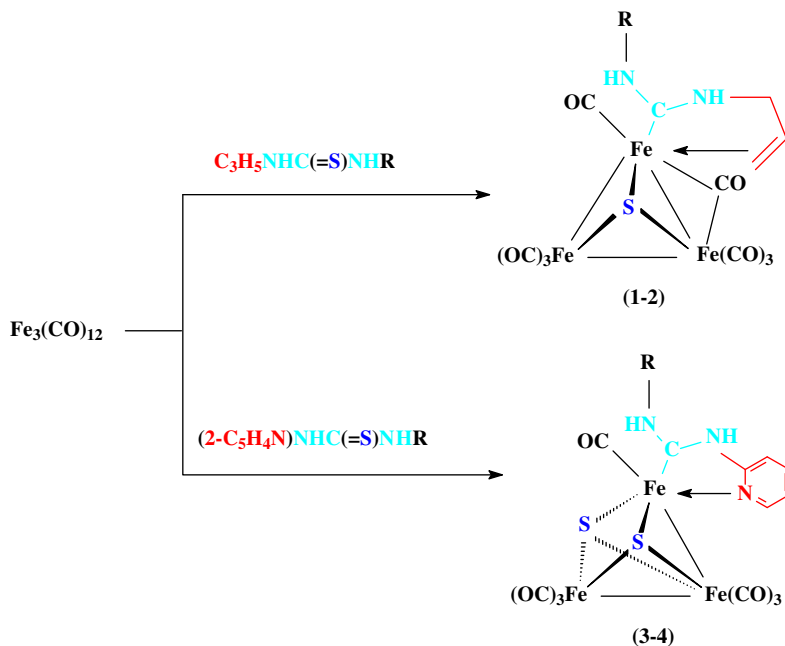
	13	14	15	16	17	18-H <sub>2</sub> O	
Formula	C <sub>24</sub> H <sub>12</sub> Fe <sub>5</sub> N <sub>4</sub> O <sub>12</sub> S <sub>3</sub>	C <sub>23</sub> H <sub>10</sub> Fe <sub>5</sub> N <sub>4</sub> O <sub>12</sub> S <sub>3</sub>	C <sub>21</sub> H <sub>11</sub> Fe <sub>5</sub> N <sub>5</sub> O <sub>12</sub> S <sub>2</sub>	C <sub>18</sub> H <sub>12</sub> Fe <sub>3</sub> N <sub>2</sub> O <sub>8</sub> Se	C <sub>18</sub> H <sub>10</sub> Fe <sub>3</sub> N <sub>4</sub> O <sub>7</sub> Se <sub>2</sub>	C <sub>20</sub> H <sub>15</sub> Fe <sub>3</sub> N <sub>3</sub> O <sub>9</sub> Se <sub>2</sub>	
Fw	923.81	909.78	872.76	630.81	719.77	766.82	
Cryst system	Monoclinic	Monoclinic	Monoclinic	Monoclinic	Monoclinic	Monoclinic	
Space group	<i>C</i> 2/ <i>c</i>	<i>P</i> 2 <sub>1</sub> / <i>c</i>	<i>P</i> 2 <sub>1</sub> / <i>c</i>	<i>P</i> 2 <sub>1</sub> / <i>n</i>	<i>P</i> 2 <sub>1</sub> / <i>c</i>	<i>P</i> 2 <sub>1</sub> 2 <sub>1</sub> 2 <sub>1</sub>	
<i>a</i> (Å)	19.889(2)	9.9502(13)	18.6451(11)	10.1261(16)	9.5441(15)	11.4381(13)	
<i>b</i> (Å)	18.9234(17)	17.0271(16)	19.0373(14)	18.048(2)	18.1393(17)	13.8261(16)	
<i>c</i> (Å)	18.4043(9)	21.6771(11)	18.1761(18)	11.9116(18)	13.872(2)	17.9465(13)	
<i>a</i> (°)	90.00	90.00	90.00	90.00	90.00	90.00	
<i>β</i> (°)	107.859(2)	115.087(2)	91.8298(14)	95.1957(13)	103.006(3)	90.00	
<i>γ</i> (°)	90.00	90.00	90.00	90.00	90.00	90.00	
<i>V</i> (Å <sup>3</sup> )	6593.0(9)	3326.2(6)	6448.4(9)	2168.0(5)	2340.0(5)	2838.1(5)	
<i>Z</i>	8	4	8	4	4	4	
<i>D<sub>c</sub></i> (g/cm <sup>-3</sup> )	1.861	1.817	1.798	1.933	2.043	1.795	
<i>μ</i> /mm <sup>-1</sup>	2.402	2.379	2.449	3.707	4.993	4.127	
<i>F</i> (0 0 0)	3664	1800	3456	1240	1392	1496	
Index ranges	-25 ≤ <i>h</i> ≤ 25 -24 ≤ <i>k</i> ≤ 24 -23 ≤ <i>l</i> ≤ 23	-11 ≤ <i>h</i> ≤ 12 -22 ≤ <i>k</i> ≤ 22 -27 ≤ <i>l</i> ≤ 28	-24 ≤ <i>h</i> ≤ 24 -24 ≤ <i>k</i> ≤ 23 -23 ≤ <i>l</i> ≤ 23	-13 ≤ <i>h</i> ≤ 12 -23 ≤ <i>k</i> ≤ 23 -15 ≤ <i>l</i> ≤ 15	-12 ≤ <i>h</i> ≤ 12 -23 ≤ <i>k</i> ≤ 23 -15 ≤ <i>l</i> ≤ 17	-14 ≤ <i>h</i> ≤ 14 -17 ≤ <i>k</i> ≤ 17 -22 ≤ <i>l</i> ≤ 23	
Measured data	28,738	28,418	55,807	18,732	20,191	24,730	
Unique data	7571	7609	14,884	4983	5370	6462	
Data [ <i>I</i> > 2σ( <i>I</i> )]	5584	5627	4440	3922	3973	4590	
<i>R</i> <sub>int</sub>	0.041	0.034	0.139	0.045	0.060	0.057	
<i>θ</i> <sub>max</sub> (°)	27.5	27.5	27.7	27.5	27.5	27.5	
<i>R</i> <sub>1</sub>	445	430	775	297	315	363	
<i>wR</i> <sub>2</sub>	0.0301	0.0348	0.0794	0.0290	0.0329	0.0365	
GOF	0.0717	0.1022	0.2283	0.0748	0.0787	0.0797	
GOF	1.00	1.06	0.87	1.02	1.02	1.01	
Peak/hole	0.42/-0.32	1.18/-0.32	1.23/-1.46	0.41/-0.40	0.39/-0.40	0.48/-0.37	

$Z = 8$ ,  $V = 5191.7(9) \text{ \AA}^3$ ;  $D_c = 1.671 \text{ gcm}^{-3}$ ;  $\mu(\text{Mo-K}\alpha) = 1.863 \text{ mm}^{-1}$ ;  $\lambda = 0.71073 \text{ \AA}$ ;  $T = 296 \text{ K}$ . For **8** and **11**, a  $\text{CH}_2\text{Cl}_2$  molecule is disordered over two positions (0.72/0.28, **8**; 0.55/0.45, **11**). Additionally, the  $\text{CH}_3\text{OC}_6\text{H}_4$  group of **11** is also disordered over two positions (0.52/0.48). As for **14**, the residual electron density at (0.1672, 0.9206, 0.2831) is  $1.18\text{e}/\text{\AA}^3$  and  $1.36 \text{ \AA}$  away from S1, which does not mean the presence of  $\text{H}_2\text{O}$ . For **18**, a water molecule is disordered over two positions (0.51/0.49). Plots of clusters are drawn using PLATON [51]. Details of crystal data, data collections, and structure refinements are listed in tables 1–3.

### 3. Results and discussion

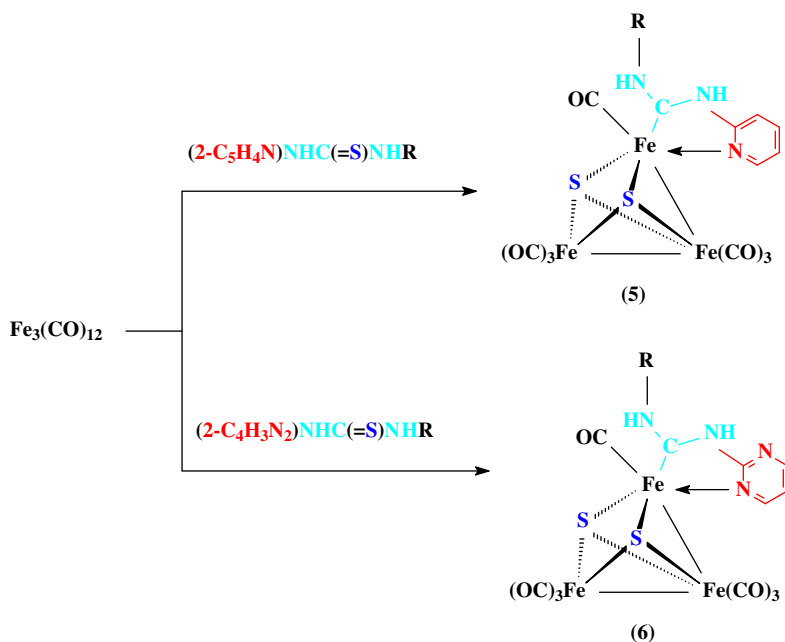
#### 3.1. Syntheses and characterizations of clusters

The reaction of  $\text{C}_3\text{H}_5\text{NHC}(=\text{S})\text{NHPH}$  with  $\text{Fe}_3(\text{CO})_{12}$  in a molar ratio of 1:1 affords  $(\mu_3\text{-S})\text{Fe}_3(\text{CO})_7(\mu\text{-CO})(\kappa^3\text{C},\text{C},\text{C}\text{-C}_3\text{H}_5\text{NHCNHPH})$  (**1**). Similarly,  $\text{C}_3\text{H}_5\text{NHC}(=\text{S})\text{NH}(4\text{-H}_2\text{NC}_6\text{H}_4)$  reacts with  $\text{Fe}_3(\text{CO})_{12}$  to produce  $(\mu_3\text{-S})\text{Fe}_3(\text{CO})_7(\mu\text{-CO})(\kappa^3\text{C},\text{C},\text{C}\text{-C}_3\text{H}_5\text{NHCNH}(4\text{-H}_2\text{NC}_6\text{H}_4))$  (**2**) (scheme 1). Unlike the above thioureas, the reaction of  $(2\text{-C}_5\text{H}_4\text{N})\text{NHC}(=\text{S})\text{NHN}=\text{HCPh}$  with  $\text{Fe}_3(\text{CO})_{12}$  or  $\text{Fe}_2(\text{CO})_9$  in a molar ratio of 1:3 gives  $(\mu_3\text{-S})_2\text{Fe}_3(\text{CO})_7(\kappa^2\text{N},\text{C}\text{-}(2\text{-C}_5\text{H}_4\text{N})\text{NHCNHN}=\text{HCPh})$  (**3**). The reaction of  $(2\text{-C}_5\text{H}_4\text{N})\text{NHC}(=\text{S})\text{NHN}=\text{HC}(4\text{-CH}_3\text{C}_6\text{H}_4)$  with  $\text{Fe}_2(\text{CO})_9$  proceeds in a similar fashion to result in the formation of  $(\mu_3\text{-S})_2\text{Fe}_3(\text{CO})_7(\kappa^2\text{N},\text{C}\text{-}(2\text{-C}_5\text{H}_4\text{N})\text{NHCNHN}=\text{HC}(4\text{-CH}_3\text{C}_6\text{H}_4))$  (**4**). Reaction of  $(2\text{-C}_5\text{H}_4\text{N})\text{NHC}(=\text{S})\text{NHC}(=\text{O})\text{Ph}$  with  $\text{Fe}_3(\text{CO})_{12}$  forms  $(\mu_3\text{-S})_2\text{Fe}_3(\text{CO})_7(\kappa^2\text{N},\text{C}\text{-}(2\text{-C}_5\text{H}_4\text{N})\text{NHCNHC}$

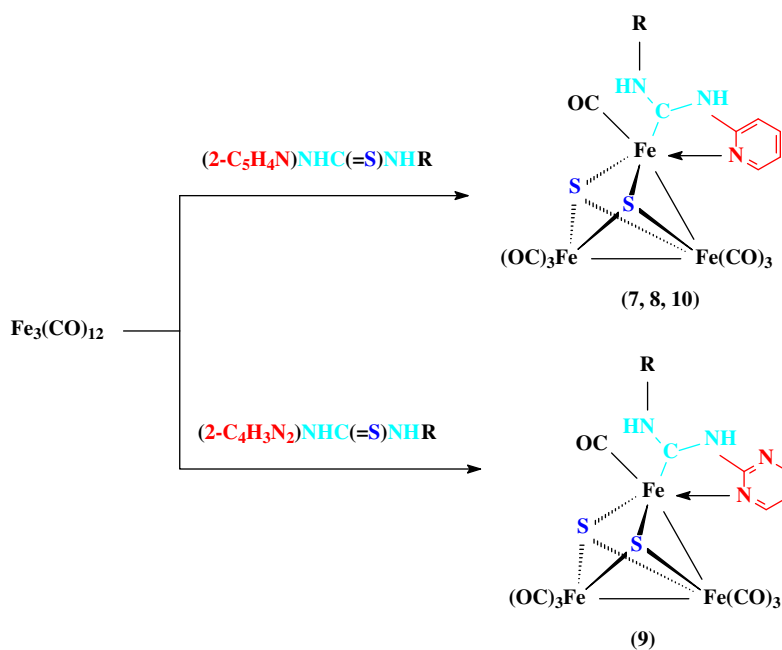


Scheme 1. Syntheses of **1–4** (**1**, R,  $\text{C}_6\text{H}_5$ ; **2**, R,  $4\text{-H}_2\text{NC}_6\text{H}_4$ ; **3**, R,  $\text{N}=\text{CHC}_6\text{H}_5$ ; **4**, R,  $\text{N}=\text{CH}(4\text{-CH}_3\text{C}_6\text{H}_4)$ ).

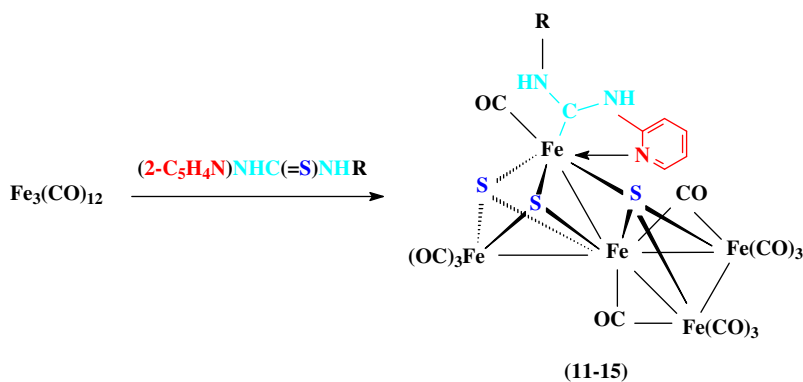
(=O)Ph) (**5**). Interestingly, (2-C<sub>4</sub>H<sub>3</sub>N<sub>2</sub>)NHC(=S)NHC(=O)Ph offers (μ<sub>3</sub>-S)<sub>2</sub>Fe<sub>3</sub>(CO)<sub>7</sub>(κ<sup>2</sup>N,C-(2-C<sub>4</sub>H<sub>3</sub>N<sub>2</sub>)NHCNHC(=O)Ph) (**6**) as well as Fe<sub>3</sub>(CO)<sub>8</sub>(μ-CO)<sub>2</sub>(κ<sup>2</sup>N,C-(2-C<sub>4</sub>H<sub>3</sub>N<sub>2</sub>)NHCNHC(=O)Ph) (scheme 2). In particular, the reaction of (2-C<sub>5</sub>H<sub>4</sub>N)NHC(=S)NH<sub>2</sub> with Fe<sub>3</sub>(CO)<sub>12</sub> provides (μ<sub>3</sub>-S)<sub>2</sub>Fe<sub>3</sub>(CO)<sub>7</sub>(κ<sup>2</sup>N,C-(2-C<sub>5</sub>H<sub>4</sub>N)NHCNH<sub>2</sub>) (**7**) (scheme 3), which can also be almost quantitatively generated from the reaction of **5** with KOH in THF. In contrast, the reactions of GNHC(=S)NHPPh with Fe<sub>3</sub>(CO)<sub>12</sub> have been investigated and clusters of (μ<sub>3</sub>-S)<sub>2</sub>Fe<sub>3</sub>(CO)<sub>7</sub>(κ<sup>2</sup>N,C-GNHCNHPPh) (**8**, G = 2-C<sub>5</sub>H<sub>4</sub>N; **9**, G = 2-C<sub>4</sub>H<sub>3</sub>N<sub>2</sub>) are obtained. Similarly, the reaction of (2-C<sub>5</sub>H<sub>4</sub>N)NHC(=S)NH(2-CH<sub>3</sub>C<sub>6</sub>H<sub>4</sub>) with Fe<sub>3</sub>(CO)<sub>12</sub> forms (μ<sub>3</sub>-S)<sub>2</sub>Fe<sub>3</sub>(CO)<sub>7</sub>(κ<sup>2</sup>N,C-(2-C<sub>5</sub>H<sub>4</sub>N)NHCNH(2-CH<sub>3</sub>C<sub>6</sub>H<sub>4</sub>)) (**10**). Seemingly, the thioureas with N-heterocycles are prone to produce the S<sub>2</sub>Fe<sub>3</sub>-type clusters. However, to our surprise, the reaction of (2-C<sub>5</sub>H<sub>4</sub>N)NHC(=S)NH(2-CH<sub>3</sub>OC<sub>6</sub>H<sub>4</sub>) with Fe<sub>3</sub>(CO)<sub>12</sub> in a molar ratio of 1:1.5 generates an unprecedented S<sub>3</sub>Fe<sub>5</sub>-type cluster, (μ<sub>3</sub>-S)<sub>2</sub>(μ<sub>4</sub>-S)Fe<sub>5</sub>(CO)<sub>10</sub>(μ-CO)<sub>2</sub>(κ<sup>2</sup>N,C-(2-C<sub>5</sub>H<sub>4</sub>N)NHCNH(2-CH<sub>3</sub>OC<sub>6</sub>H<sub>4</sub>)) (**11**) (scheme 4). Reactions of (2-C<sub>5</sub>H<sub>4</sub>N)NHC(=S)NHR with Fe<sub>3</sub>(CO)<sub>12</sub> also yield (μ<sub>3</sub>-S)<sub>2</sub>(μ<sub>4</sub>-S)Fe<sub>5</sub>(CO)<sub>10</sub>(μ-CO)<sub>2</sub>(κ<sup>2</sup>N,C-(2-C<sub>5</sub>H<sub>4</sub>N)NHCNHR) (**12**, R = 2-H<sub>2</sub>NC<sub>6</sub>H<sub>4</sub>; **13**, R = 4-H<sub>2</sub>NC<sub>6</sub>H<sub>4</sub>; **14**, R = 2-C<sub>5</sub>H<sub>4</sub>N). More interestingly, the reaction of (2-C<sub>5</sub>H<sub>4</sub>N)NHC(=S)NHC<sub>3</sub>H<sub>5</sub> with Fe<sub>3</sub>(CO)<sub>12</sub> gives (μ<sub>3</sub>-S)<sub>2</sub>(μ<sub>4</sub>-S)Fe<sub>5</sub>(CO)<sub>10</sub>(μ-CO)<sub>2</sub>(κ<sup>2</sup>N,C-(2-C<sub>5</sub>H<sub>4</sub>N)NHCNHC<sub>3</sub>H<sub>5</sub>) (**15**). In order to compare the reactivity toward iron carbonyls between thioureas and selenoureas, reactions of three selenoureas with Fe<sub>3</sub>(CO)<sub>12</sub> have been carried out. The reaction of C<sub>3</sub>H<sub>5</sub>NHC(=Se)NHPPh with Fe<sub>3</sub>(CO)<sub>12</sub> affords (μ<sub>3</sub>-Se)Fe<sub>3</sub>(CO)<sub>7</sub>(μ-CO)(κ<sup>3</sup>C,C-C<sub>3</sub>H<sub>5</sub>NHCNHPPh) (**16**) as well as [(κ<sup>2</sup>N,C-PhN=CNHC<sub>3</sub>H<sub>5</sub>)Fe<sub>2</sub>(CO)<sub>6</sub>(μ<sub>4</sub>-Se)Fe<sub>2</sub>(CO)<sub>6</sub>]<sub>2</sub>(μ<sub>4</sub>-Se) (scheme 5). Like (2-C<sub>4</sub>H<sub>3</sub>N<sub>2</sub>)NHC(=S)NHPPh, (2-C<sub>4</sub>H<sub>3</sub>N<sub>2</sub>)NHC(=Se)NHPPh reacts with Fe<sub>3</sub>(CO)<sub>12</sub> to form (μ<sub>3</sub>-Se)<sub>2</sub>Fe<sub>3</sub>(CO)<sub>7</sub>(κ<sup>2</sup>N,C-(2-C<sub>4</sub>H<sub>3</sub>N<sub>2</sub>)NHCNHPPh) (**17**) and (2-C<sub>5</sub>H<sub>4</sub>N)NHC(=Se)NHPPh provides (μ<sub>3</sub>-Se)<sub>2</sub>Fe<sub>3</sub>(CO)<sub>7</sub>(κ<sup>2</sup>N,C-(2-C<sub>5</sub>H<sub>4</sub>N)NHCNHPPh). In sharp contrast with (2-C<sub>5</sub>H<sub>4</sub>N)NHC(=S)NH(2-CH<sub>3</sub>OC<sub>6</sub>H<sub>4</sub>),



Scheme 2. Syntheses of **5** and **6** (**5**, R, COPh; **6**, R, COPh).

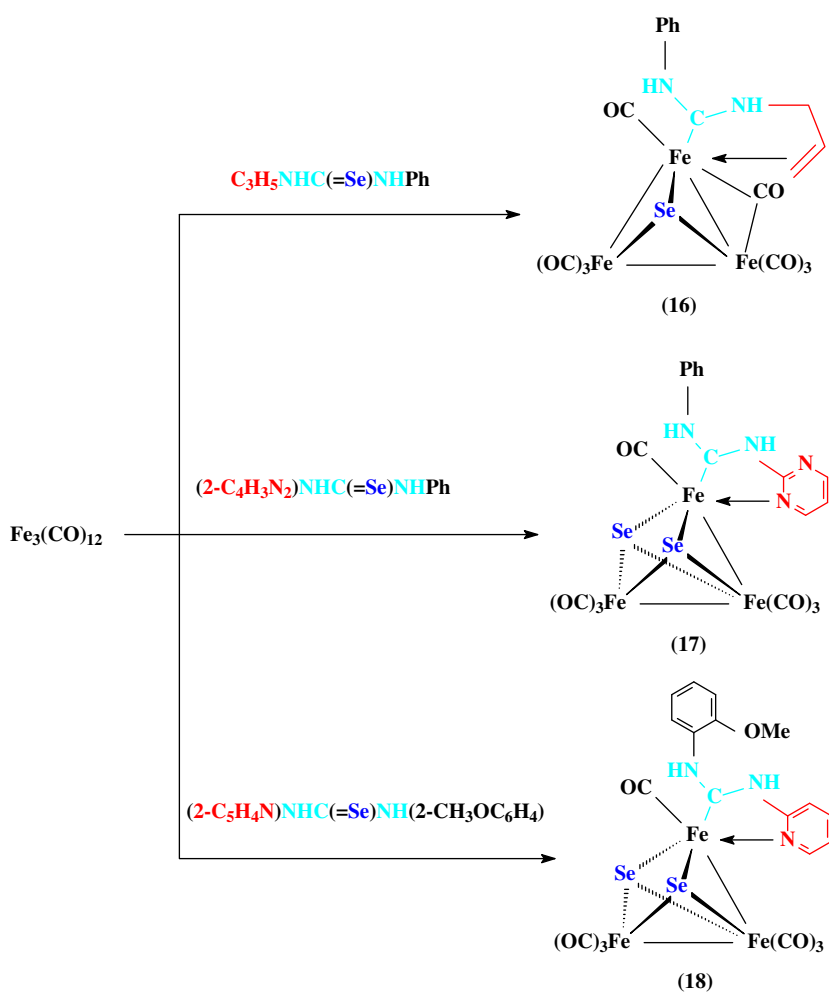


Scheme 3. Syntheses of **7–10** (**7**, R, H; **8**, R,  $\text{C}_6\text{H}_5$ ; **9**, R,  $\text{C}_6\text{H}_5$ ; **10**, R,  $2\text{-CH}_3\text{C}_6\text{H}_4$ ).



Scheme 4. Syntheses of **11–15** (**11**, R,  $2\text{-CH}_3\text{OC}_6\text{H}_4$ ; **12**, R,  $2\text{-H}_2\text{NC}_6\text{H}_4$ ; **13**, R,  $4\text{-H}_2\text{NC}_6\text{H}_4$ ; **14**, R,  $2\text{-C}_5\text{H}_4\text{N}$ ; **15**, R,  $\text{C}_3\text{H}_5$ ).

$(2\text{-C}_5\text{H}_4\text{N})\text{NHC}(=\text{Se})\text{NH}(2\text{-CH}_3\text{OC}_6\text{H}_4)$  yields  $(\mu_3\text{-Se})_2\text{Fe}_3(\text{CO})_7(\kappa^2N,C\text{-}(2\text{-C}_5\text{H}_4\text{N})\text{NHCNH}(2\text{-CH}_3\text{OC}_6\text{H}_4))$  (**18**). Although mechanistic details have not been explored, we propose a possible mechanism to shed light on formation of these new Fe/S clusters with chelating carbene ligands [53] (chart 1): thiourea  $\text{GNHC}(=\text{S})\text{NHR}$  (G = coordination group:  $2\text{-C}_5\text{H}_4\text{N}$ ,  $2\text{-C}_4\text{H}_3\text{N}_2$ ,  $\text{CH}_2\text{CH}=\text{CH}_2$ ) reacts with iron carbonyls to produce **M1** with loss of CO; **M1** undergoes a thermal rearrangement to afford an  $\text{SFe}_3$ -type cluster or via an S transfer leads to an unstable derivative (**M2**) of  $\text{Fe}_3(\text{CO})_{12}$  with a chelating carbene ligand and an  $\text{S}_2\text{Fe}_3$ -type

Scheme 5. Syntheses of **16**–**18**.

cluster, or reacts with  $\text{Fe}_3(\text{CO})_{12}$  to offer **M2** and  $\text{SFe}_3(\text{CO})_{10}$  (**M3**) [54]; **M3** reacts with the  $\text{S}_2\text{Fe}_3$ -type cluster to form an  $\text{S}_3\text{Fe}_5$ -type cluster with  $\text{Fe}(\text{CO})_5$  being released, whereas  $\text{S}_2\text{Fe}_3(\text{CO})_9$  is generated by self-condensation of **M3**. The green structurally characterized **M2**,  $\text{Fe}_3(\text{CO})_8(\mu\text{-CO})_2(\kappa^2\text{N},\text{C}\text{-}(2\text{-C}_4\text{H}_3\text{N}_2)\text{NHCNHC}(=\text{O})\text{Ph})$ , and yellow  $\text{Fe}(\text{CO})_5$  detected support these hypotheses. Naturally, the isolation of the above  $\text{Se}_3\text{Fe}_8$  cluster hints that besides possible intermediates  $(\text{GNHCSeNHR})\text{Fe}_3(\text{CO})_9$ ,  $(\text{GNHCNHR})\text{Fe}_3(\text{CO})_{10}$ , and  $\text{SeFe}_3(\text{CO})_{10}$  [55], being similar to **M1**, **M2**, and **M3** (drawn in chart 1), selenourea GNHC(=Se)NHR (G = coordination group:  $2\text{-C}_5\text{H}_4\text{N}$ ,  $2\text{-C}_4\text{H}_3\text{N}_2$ ,  $\text{CH}_2\text{CH}=\text{CH}_2$ ) reacts through another pathway, via an unstable intermediate  $(\mu\text{-HSe})\text{Fe}_2(\text{CO})_6(\kappa^2\text{C},\text{N}\text{-GNHC}=\text{NR})$ , to generate an  $\text{Se}_3\text{Fe}_8$  cluster [28(d)].

These new clusters have been characterized by FT-IR,  $^1\text{H}$  NMR,  $^{13}\text{C}\{^1\text{H}\}$  NMR, and elemental analyses. In the IR spectra, the NH vibration is at  $3026\text{--}3366\text{ cm}^{-1}$ . The terminal carbonyl groups show two to four strong absorptions from  $1906$  to  $2070\text{ cm}^{-1}$ . The



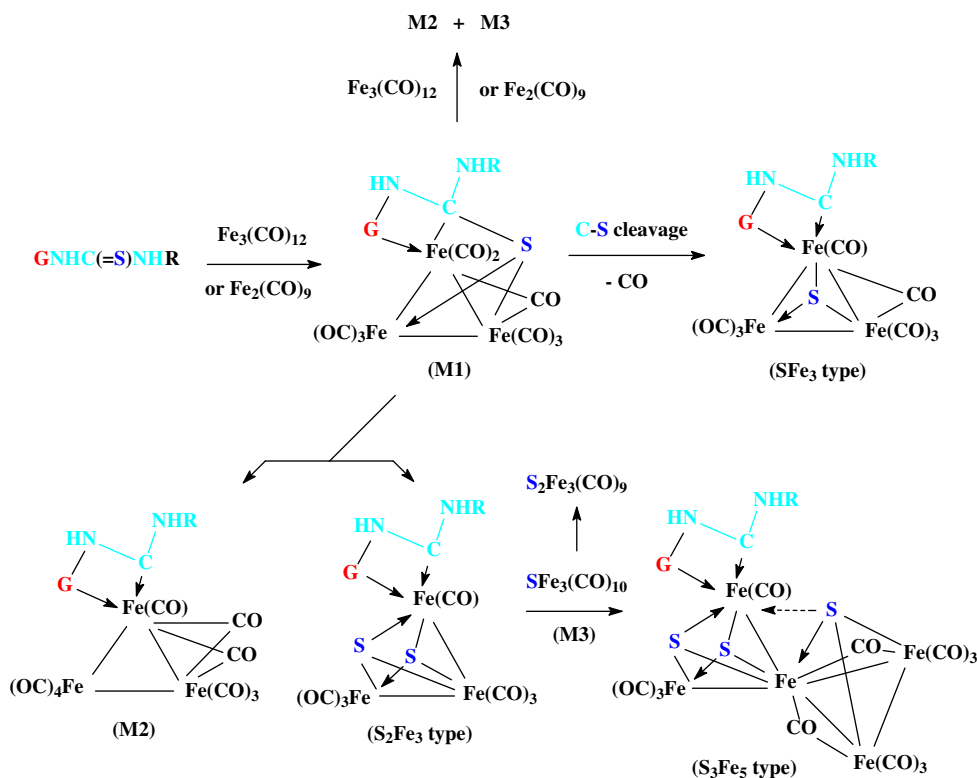
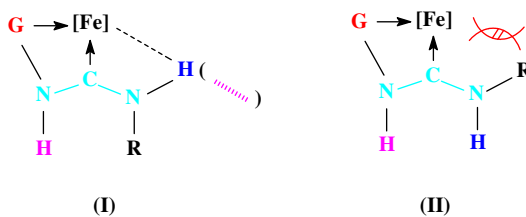


Chart 1. Proposed mechanism for Fe/S clusters.

bridging carbonyl group(s) occur(s) at 1820–1863  $\text{cm}^{-1}$  for  $\text{SFe}_3$ ,  $\text{S}_3\text{Fe}_5$ , and  $\text{SeFe}_3$  clusters (**1**, 1862 (m); **2**, 1863 (m); **11**, 1829 (m); **12**, 1820 (m); **13**, 1830 (m); **14**, 1832 (m); **15**, 1839 (m); **16**, 1856 (m)  $\text{cm}^{-1}$ ). These data strongly support the seemingly unacceptably long Fe-carbonyl bonds determined by X-ray crystallography (see below). In the  $^1\text{H}$  NMR spectra, the NH group, which was verified by  $\text{D}_2\text{O}$  exchange, shows a slightly upfield shift by comparison with the corresponding thiourea and selenourea. The very low-field signals for **5** ( $\delta$  13.05), **6** ( $\delta$  13.26), and **14** ( $\delta$  14.48) result from strong classical hydrogen bonds ( $\text{N}-\text{H}\cdots\text{O}$ ,  $\text{N}-\text{H}\cdots\text{O}$ , and  $\text{N}-\text{H}\cdots\text{N}$ ). In the  $^{13}\text{C}$  NMR spectra, the carbene C is at

Chart 2. Two conformations of chelating  $N,N'$ -diaminocarbenes. Dashed lines indicate hydrogen bonds.

147–159 ppm. The signals from the CO groups reveal that the five types of  $\text{SFe}_3$ ,  $\text{S}_2\text{Fe}_3$ ,  $\text{S}_3\text{Fe}_5$ ,  $\text{SeFe}_3$ , and  $\text{Se}_2\text{Fe}_3$  clusters are all fluxional in solution.

### 3.2. Molecular structures of clusters

These new clusters including green  $\text{Fe}_3(\text{CO})_8(\mu\text{-CO})_2(\kappa^2\text{N},\text{C}-(2\text{-C}_4\text{H}_3\text{N}_2)\text{NHCNHC}(\text{=O})\text{Ph})$  and black  $[(\kappa^2\text{N},\text{C}-\text{PhN}=\text{CNHC}_3\text{H}_5)\text{Fe}_2(\text{CO})_6(\mu_4\text{-Se})\text{Fe}_2(\text{CO})_6]_2(\mu_4\text{-Se})$  (see Supplementary Data) have been structurally determined by X-ray crystallography. However, for clarity, only molecular structures of **1**, **4**, **6**, **7**, **9**, **11**, **13**, **14**, **16**, and **17** are discussed below.

Cluster **1** (figure 1) consists of a triangular core of irons with three Fe–Fe bonds capped by a sulfide ligand, which is 1.5975(6) Å from the triiron plane [54]. The sulfide ligand symmetrically links three Fe atoms with Fe–S bond lengths averaging 2.197(6) Å, compared to the Fe–S bond length of 2.21(1) Å in  $\text{Fe}_3(\text{CO})_9(\mu_3\text{-CO})(\mu_3\text{-S})$  [54(a)]. Fe1 has one terminal carbonyl and chelating carbene ligand, while Fe2 and Fe3 each bear three terminal carbonyls. The carbonyl on Fe1 is obviously bent toward Fe3 with a 171.7(2)° angle of Fe1–C1–O1. The Fe3···C1 distance of 2.765(3) Å suggests an intramolecular contact between the two atoms [ $r$ , covalent radius;  $R$ , van der Waals radius;  $r(\text{Fe}) = 1.45$ ,  $r(\text{C}) = 0.68$ ,  $r(\text{Fe}) + r(\text{C}) = 2.13$  Å;  $R(\text{Fe}) = 2.14$ ,  $R(\text{C}) = 1.70$ ,  $R(\text{Fe}) + R(\text{C}) = 3.84$  Å] [51]. The semibridging carbonyl binds Fe1 and Fe2 [Fe1–C8, 1.841(2) Å; Fe2–C8, 2.231(2) Å; Fe1–C8–O8, 154.12(18)°; Fe2–C8–O8, 125.25(16)°; Fe1–C8–Fe2, 80.35(8)°] and lies approximately *trans* to the carbene C12 [C8–Fe1–C12, 160.49(9)°]. The existence of the

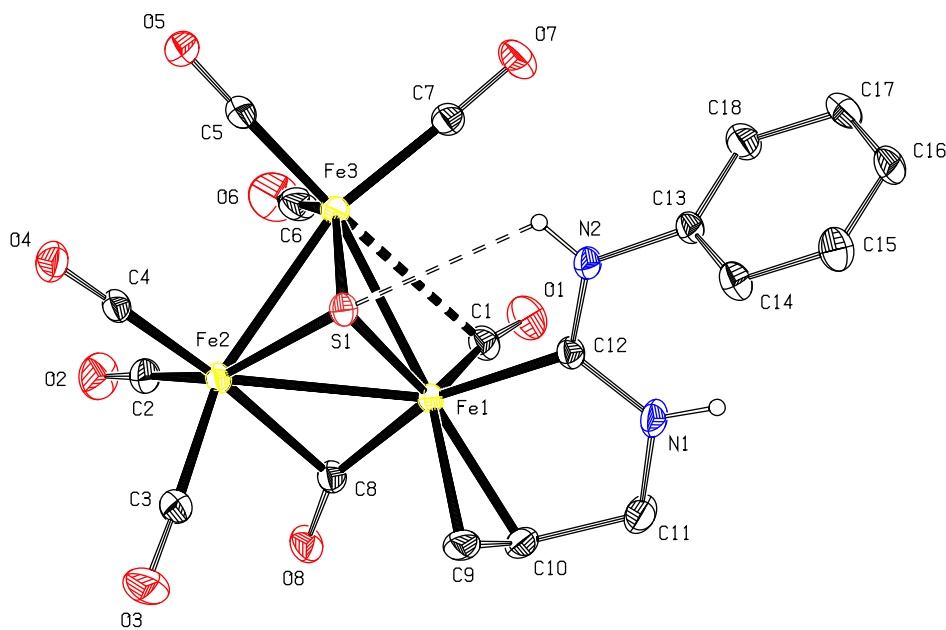


Figure 1. Molecular structure of **1**. Selected geometric parameters (Å, °): Fe1–Fe2, 2.6442(4); Fe2–Fe3, 2.5751(4); Fe1–Fe3, 2.6156(4); Fe1–S1, 2.1915(6); Fe2–S1, 2.1924(6); Fe3–S1, 2.2071(6); Fe1–C8, 1.841(2); Fe2–C8, 2.231(2); Fe1–C9, 2.115(2); Fe1–C10, 2.116(2); C9–C10, 1.394(3); Fe1–C12, 1.9976(19); Fe1–C1–O1, 171.7(2).

semibridging carbonyl is due to steric congestion from the chelating carbene ligand and governed by the 18-electron rule. Notably, the Fe–C<sub>semibridging</sub> bond of 2.231(2) Å is significantly longer than that of Fe<sub>3</sub>(CO)<sub>8</sub>(μ-CO)(μ<sub>3</sub>-S)(PPh<sub>2</sub>CC<sup>t</sup>Pr) [Fe1–CO, 1.895(5); Fe2–CO, 2.142(6) Å; IR, 1866 (w) cm<sup>-1</sup>] [54(b)]. Against expectation, the bridged Fe1–Fe2 bond of 2.6442(4) Å is longer than the other two [Fe2–Fe3, 2.5751(4) Å; Fe1–Fe3, 2.6156(4) Å]. For comparison, three Fe–Fe bond lengths of the reported complex are 2.582(1), 2.591(2), and 2.620(1) Å. The sum of the bond angles about C12 is 360.00(16)° [Fe1–C12–N1, 116.26(15); Fe1–C12–N2, 126.25(15); N1–C12–N2, 117.49(18)°], indicating that the carbene C12 is sp<sup>2</sup>-hybridized. The Fe1–C12 bond length of 1.998(2) Å in **1** is typical of an Fe–C single bond, falling near the normal range of 2.0–2.2 Å [25(b), 56, 57] and almost equal to the Fe–C<sub>carbene</sub> bond lengths of 2.007(5) Å in IMFe(CO)<sub>4</sub> (IM = 1,3-dimethylimidazol-2-ylidene) [58(a)], 1.992(2) Å in IMesFe(CO)<sub>4</sub> (IMes = 1,3-dimesitylimidazol-2-ylidene) [58(b)], and 1.992(3) Å in CpFe(CO)(Ph<sub>2</sub>PCH<sub>2</sub>CH<sub>2</sub>CH<sub>2</sub>HNCN<sup>n</sup>Hex)<sub>2</sub>I, but longer than the 1.958(3) Å bond observed in CpFe(CO)(<sup>t</sup>Bu<sub>2</sub>PCH<sub>2</sub>CH<sub>2</sub>CH<sub>2</sub>HNCNH<sup>n</sup>Bu)I [58(c)]. The C12–N1 and C12–N2 bond lengths of 1.322(3) and 1.335(3) Å suggest π-electrons delocalizing over the N1–C12–N2 group [53(f), 59]. In this case, the carbene C12 functions only as an *n* donor. The bond lengths of Fe1–C9 and Fe1–C10 [2.115(2) and 2.116(2) Å] show that they are single bonds, whereas the C9–C10 bond of 1.394(3) Å is of some double bond character. Therefore, the allyl group is best described as a κ<sup>3</sup>C,C mode and the chelating carbene ligand is a four-electron donor in a κ<sup>3</sup>C,C,C fashion. The Fe1C9C10 plane is nearly perpendicular to the carbene CN<sub>2</sub> plane, forming a dihedral angle of 89.6(2)°. The carbene CN<sub>2</sub> plane makes a dihedral angle of 71.91(11)° with the phenyl plane. This type of clusters (**1** and **2**) with chelating carbene ligands, (μ<sub>3</sub>-S)Fe<sub>3</sub>(CO)<sub>7</sub>(μ-CO)L<sub>2</sub> (L<sub>2</sub> = C<sub>carbene</sub>–N<sub>heterocycle</sub> ligand), is unprecedented.

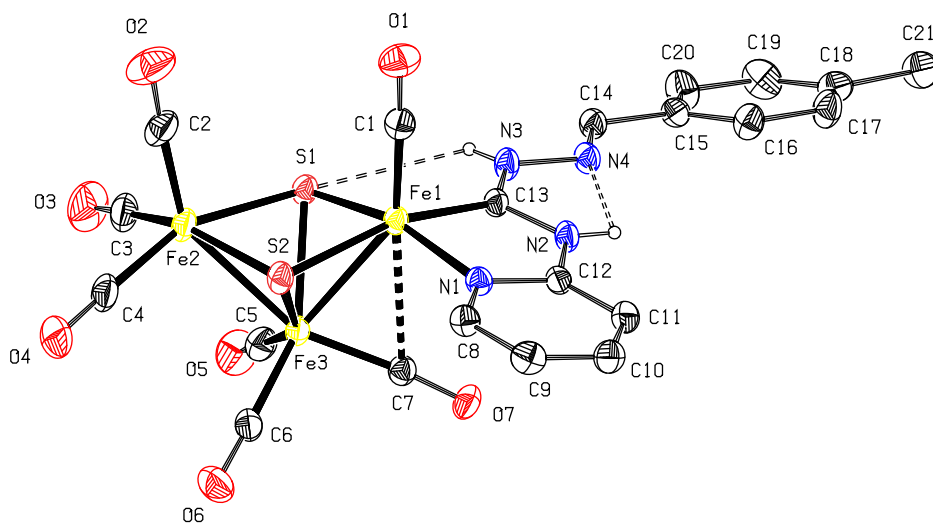


Figure 2. Molecular structure of **4**. Selected geometric parameters (Å, °): Fe1–N1, 2.004(3); Fe1–Fe3, 2.6319(8); Fe2–Fe3, 2.5494(8); Fe1–S1, 2.2025(11); Fe1–S2, 2.2305(9); Fe2–S1, 2.2589(10); Fe2–S2, 2.2538(11); Fe3–S1, 2.2696(11); Fe3–S2, 2.2755(12); Fe1–C13, 1.914(3); Fe1–C1, 1.736(5); Fe1···C7, 2.763(4); Fe1–Fe3–Fe2, 82.00(2); Fe3–C7–O7, 174.1(4).

As shown in figure 2, **4** contains an open triangle of Fe atoms capped by two S atoms above and below, with an Fe1–Fe3–Fe2 angle of 82.00(2)°. The S<sub>2</sub>Fe<sub>3</sub> core adopts a distorted square-pyramidal geometry similar to the previously reported cluster (μ<sub>3</sub>-S)<sub>2</sub>Fe<sub>3</sub>(CO)<sub>9</sub> [59]. In (μ<sub>3</sub>-S)<sub>2</sub>Fe<sub>3</sub>(CO)<sub>9</sub>, each sulfur on the square base triply bridges the two basal Fe(CO)<sub>3</sub> units on the same base and the third Fe(CO)<sub>3</sub> group at the apex of the pyramid, and each of the three Fe atoms obeys the 18-electron rule. Accordingly, **4** may be viewed as involving formal replacement of the two equatorial carbonyl ligands on one of the iron centers on the square base in (μ<sub>3</sub>-S)<sub>2</sub>Fe<sub>3</sub>(CO)<sub>9</sub> by a four-electron chelating carbene, viz. carbene C and pyridine N, with Fe1–C13 = 1.914(3) and Fe1–N1 = 2.004(3) Å. The carbene ligand leads to small structural effects, namely a slight increase in the triiron bond angle compared with (μ<sub>3</sub>-S)<sub>2</sub>Fe<sub>3</sub>(CO)<sub>9</sub> [81.13(2)°; 2.5903(9) and 2.5946(9) Å], and a slight increase in the Fe–Fe bond-length difference from 0.0043(9) to 0.0825(8) Å. Additionally, one of the three carbonyl ligands attached to the apical Fe takes part in a weak interaction with the carbene-substituted basal Fe from a direction *trans* to the carbonyl ligand bound to the basal Fe [Fe1···C7 = 2.763(4) Å, Fe1–C1···C7 = 175.26(15)°]. In agreement with this interaction is a significant deviation of the Fe–C–O bond angle from linearity, with carbonyl C7 bent toward Fe1 [Fe3–C7–O7 = 174.1(4)°], whereas the others are 176.5(5)–178.6(5)°. The Fe–S bonds range from 2.2025(11) to 2.2755(12) Å. Unlike **1** and **2**, because the CN<sub>2</sub> group is coplanar with the pyridine ring, the sum of the bond angles at carbene C13 is 360.0(3)° and forms a larger conjugated system, thus strengthening π back-bonding and leading to the short Fe–C<sub>carbene</sub> bonds described above.

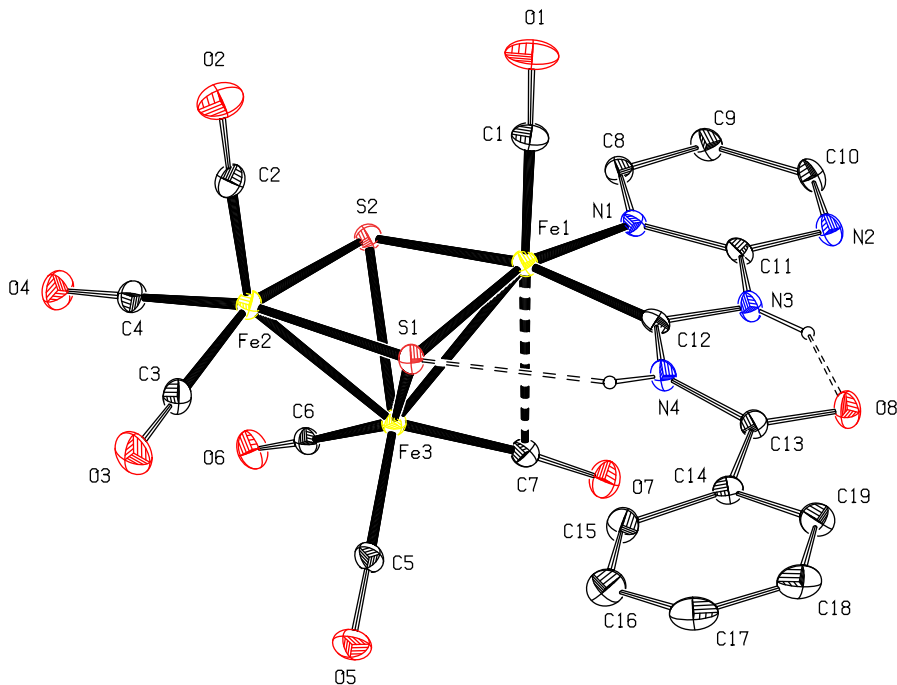


Figure 3. Molecular structure of **6**. Selected geometric parameters (Å, °): Fe1–N1, 1.985(3); Fe1–Fe3, 2.6240(9); Fe2–Fe3, 2.5712(10); Fe1–S1, 2.1902(12); Fe2–S1, 2.2401(12); Fe3–S1, 2.2615(13); Fe1–C12, 1.894(4); Fe1···C7, 2.778(6); Fe1–Fe3–Fe2, 81.23(3); Fe3–C7–O7, 173.6(4).

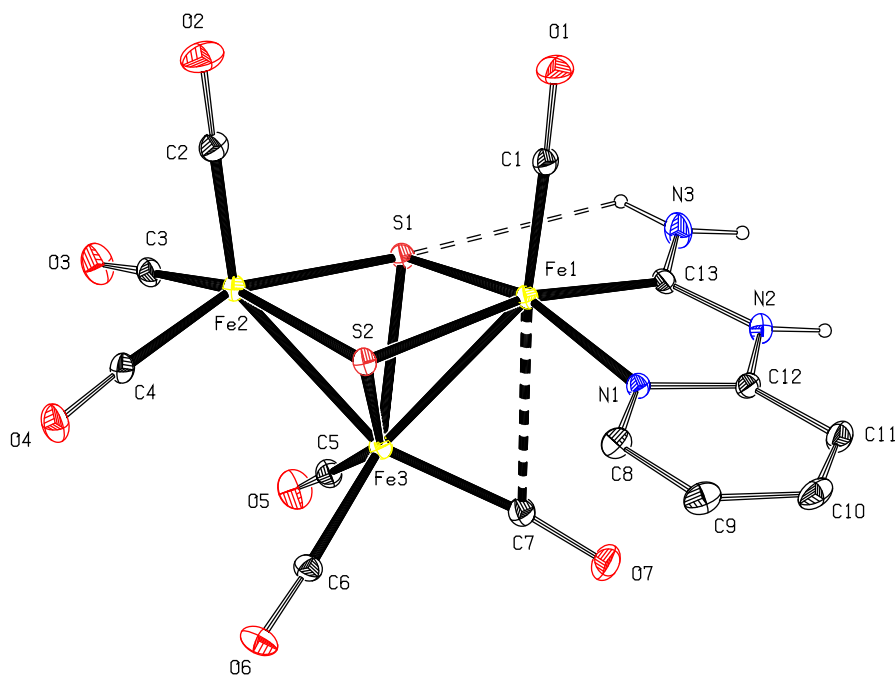


Figure 4. Molecular structure of **7**. Selected geometric parameters ( $\text{\AA}$ ,  $^\circ$ ): Fe1–N1, 2.004(2); Fe1–Fe3, 2.6377(7); Fe2–Fe3, 2.5507(6); Fe1–S1, 2.2044(8); Fe1–S2, 2.2297(8); Fe3–S1, 2.2661(8); Fe1–C13, 1.912(3); Fe1 $\cdots$ C7, 2.780(5); Fe1–Fe3–Fe2, 81.956(18); Fe3–C7–O7, 172.7(3).

Cluster **6** (figure 3) is isoelectronic to **5**. The  $\text{S}_2\text{Fe}_3$  core shows a distorted square-pyramidal geometry. The chelating carbene ligand is, via carbene C12 and pyrimidine N1, bonded to Fe1 in the equatorial position and is a four-electron donor. Of the six Fe–S bonds, the Fe2–S2 bond is the longest at 2.2773(13)  $\text{\AA}$ . The Fe1–C12 bond length of 1.894(4)  $\text{\AA}$  indicates that there exists a high degree of  $\pi$  back-donation from Fe1 to C12. In accord with this conclusion, the sum of the bond angles of Fe1–C12–N3 115.5(3), Fe1–C12–N4 126.9(3), and N2–C12–N3 117.7(4) is 360.1(3) $^\circ$ . Owing to the carbene-bound Fe being coplanar with the  $\text{CN}_2$  group and the  $\text{C}_4\text{H}_3\text{N}_2$  ring, these atoms form a larger conjugated system, resulting in the very short Fe–C<sub>carbene</sub> bond. One of three carbonyls attached to the apical Fe has a weak interaction with the carbene-substituted basal Fe [Fe1 $\cdots$ C7, 2.778(6)  $\text{\AA}$ ; C1–Fe1 $\cdots$ C7, 173.9(2) $^\circ$ ], causing a bent Fe–C–O bond angle [Fe3–C7–O7, 173.6(4) $^\circ$ ]. The triiron plane with the chelating ligand forms a dihedral angle of 87.50(11) $^\circ$ ; the chelating ligand with the NCOC plane makes a dihedral angle of 7.5(5) $^\circ$ .

Similar to **6**, **7** (figure 4) contains a triangle of Fe atoms capped by two S atoms above and below with an Fe1–Fe3–Fe2 angle of 81.956(18) $^\circ$ . Two Fe–Fe bond lengths are 2.6377(7) and 2.5507(6)  $\text{\AA}$  for Fe1–Fe3 and Fe2–Fe3, respectively. The Fe1–N1 bond length is 2.004(2)  $\text{\AA}$ . The Fe1–C13 bond length of 1.912(3)  $\text{\AA}$  is similar to that of **6**. The carbene C13 is  $\text{sp}^2$ -hybridized with an angle sum of 360.0(3) $^\circ$  [Fe1–C13–N2, 114.3(2) $^\circ$ ; Fe1–C13–N3, 129.7(3) $^\circ$ ; N2–C13–N3, 116.0(3) $^\circ$ ]. Because the carbene-bound Fe is coplanar with the  $\text{CN}_2$  group and the  $\text{C}_5\text{H}_4\text{N}$  ring, these atoms form a larger conjugated system. Unlike the

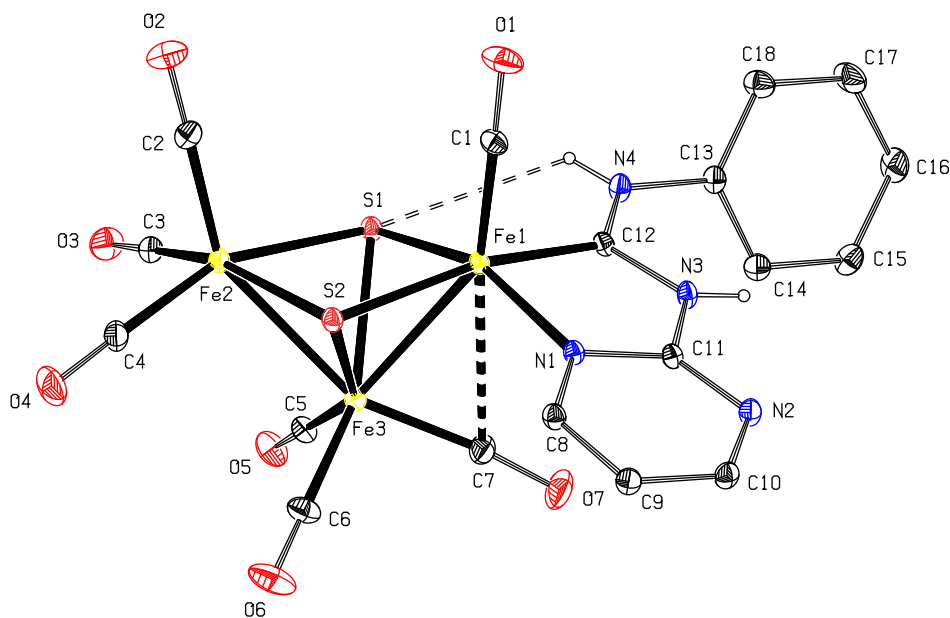


Figure 5. Molecular structure of **9**. Selected geometric parameters (Å, °): Fe1–N1, 2.002(2); Fe1–Fe3, 2.6095(6); Fe2–Fe3, 2.5448(6); Fe1–S1, 2.2023(8); Fe2–S1, 2.2562(7); Fe3–S1, 2.2752(8); Fe1–C12, 1.915(2); Fe1···C7, 2.760(3); Fe1–Fe3–Fe2, 82.899(18); Fe3–C7–O7, 173.0(3).

reported NHCs [53], this planar carbene ligand is both a good  $\sigma$ -donor and a good  $\pi$ -acceptor. The triiron plane with the chelating ligand forms a dihedral angle of 86.71(11)°. As in **4–6**, the Fe3–S bond lengths [Fe3–S1, 2.2661(8) Å; Fe3–S2, 2.2808(8) Å] in **7** are longer than the others [2.2044(8)–2.2649(8) Å]. One of the three carbonyl ligands connected to the apical Fe3 involves a weak interaction with the carbene-substituted basal Fe1 from a direction *trans* to the Fe1-bound carbonyl [Fe1···C7, 2.780(5) Å], resulting in the bent Fe3–C7–O7 bond angle [172.7(3)°].

As with **8**, **9** (figure 5) belongs to the above  $S_2Fe_3$  type with an angle of Fe1–Fe3–Fe2 being 82.899(18)°. The Fe1–C12 bond length of 1.915(2) Å is identical to that of **8** [1.915(3) Å]. The two C12–N bond lengths [C12–N3, 1.357(3); C12–N4, 1.326(3) Å] and the sum of the angles around C12 [Fe1–C12–N3, 113.87(18)°; Fe1–C12–N4, 129.5(2)°; N3–C13–N4, 116.6(2)°; 360.0(2)°] indicate that the carbene C12 adopts  $sp^2$  hybridization. With the carbene-bound Fe being coplanar with the  $CN_2$  group and the  $C_4H_3N_2$  ring, these atoms form a larger conjugated system. The triiron plane with the chelating ligand forms a dihedral angle of 78.79(7)°, clearly smaller than the angle of 89.74(7)° in **8**. The chelating ligand forms a dihedral angle of 57.83(13)° with the phenyl ring. As in **8**, one of the three carbonyl ligands linked to the apical Fe3 interacts weakly with the carbene-substituted basal Fe1 [Fe1···C7, 2.760(3) Å; C1–Fe1···C7, 171.51(12)°; Fe3–C7–O7, 173.0(3)°].

Although complexes of types  $(\mu_3-S)_2Fe_3(CO)_7L_2$  ( $L = P$  ligand) and  $(\mu_3-S)_2Fe_3(CO)_8L$  ( $L =$  carbene ligand) are known, clusters with equatorial carbene ligands are extremely rare:  $(\mu_3-S)_2Fe_3(CO)_8L$  ( $L = C_3Ph_2$  [59(d)], Fe– $C_{\text{carbene}}$ , 1.901(7) Å;  $L = C_3H_2S_2$  (dithiocarbene) [59(e)], Fe– $C_{\text{carbene}}$ , 1.948(3) Å;  $L = C_{10}H_{10}N_2S_2$  (aminothiocarbene) [59(f)], Fe– $C_{\text{carbene}}$ ,

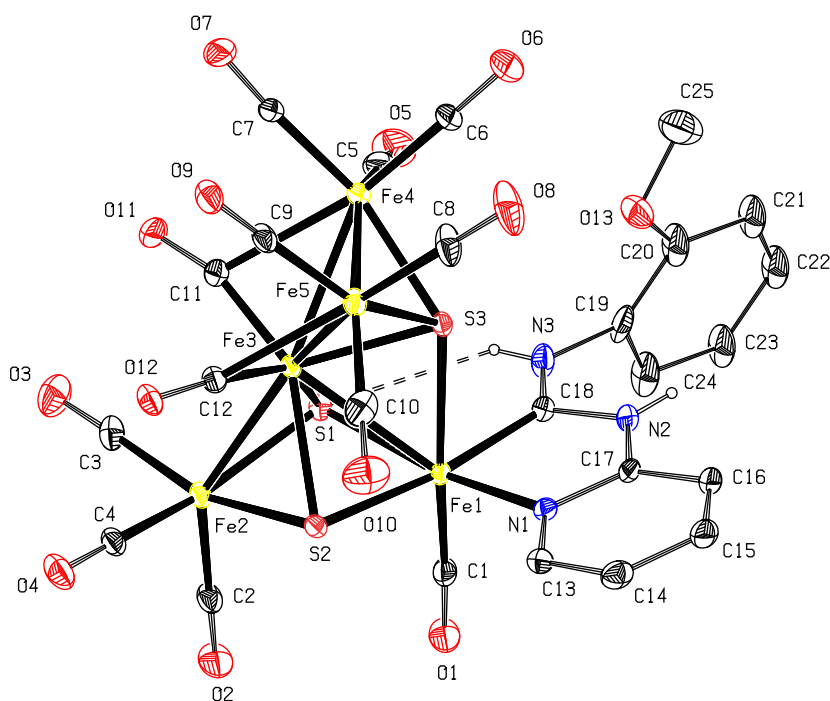


Figure 6. Molecular structure of **11**. Selected geometric parameters ( $\text{\AA}$ ,  $^\circ$ ): Fe1–Fe3, 2.7780(10); Fe2–Fe3, 2.5773(10); Fe3–Fe4, 2.6075(10); Fe3–Fe5, 2.5992(10); Fe4–Fe5, 2.6098(13); Fe1–S1, 2.2175(15); Fe1–S2, 2.2663(14); Fe1–S3, 2.5808(15); Fe1–N1, 1.997(4); Fe1–C18, 1.927(5); Fe1–Fe3–Fe2, 78.58(3); Fe3–C11–Fe4, 74.7(2); Fe3–C12–Fe5, 74.7(2); C1–Fe1–S3, 176.6(2).

1.959(4)  $\text{\AA}$ ). This type of clusters with chelating carbene ligands **3–10**,  $(\mu_3\text{-S})_2\text{Fe}_3(\text{CO})_7L_2$  ( $L_2 = \text{C}_{\text{carbene}}\text{-N}_{\text{heterocycle}}$  chelating ligand), is unprecedented.

Cluster **11** (figure 6) consists of an open triiron and a closed triiron framework sharing a vertex [60]. The two triangles are really vertical, with a dihedral angle of  $89.48(5)^\circ$  while a value in  $[(\text{PPh}_3)_2\text{N}]_2[\text{Fe}_5(\text{CO})_{14}(\mu_3\text{-S})_2]$  is  $55.08(3)^\circ$  [60(b)]. The open triiron core is capped by two S atoms above and below with a triiron angle of  $78.58(3)^\circ$ , smaller than that observed in  $(\mu_3\text{-S})_2\text{Fe}_3(\text{CO})_9$  of  $[81.13(2)^\circ]$  [59(a)]. The  $\text{S}_2\text{Fe}_3$  subcore in **11** shows a distorted square-pyramidal geometry similar to that in  $(\mu_3\text{-S})_2\text{Fe}_3(\text{CO})_9$ . The chelating carbene ligand as a four-electron donor via the carbene C18 and pyridine N1 is equatorially coordinated to the basal Fe1 with Fe1–C18 = 1.927(5)  $\text{\AA}$  and Fe1–N1 = 1.997(4)  $\text{\AA}$ . As in **3–10**, carbene C18 is  $\text{sp}^2$ -hybridized [Fe1–C18–N2,  $113.6(4)^\circ$ ; Fe1–C18–N3,  $129.1(4)^\circ$ ; N2–C18–N3,  $117.3(5)^\circ$ ;  $360.0(4)^\circ$ ]. With the carbene-bound Fe being coplanar with the  $\text{CN}_2$  group and the  $\text{C}_5\text{H}_4\text{N}$  ring, these atoms form a larger conjugated system. The chelating ligand is almost perpendicular to the Fe1–Fe3–Fe2 plane, forming a dihedral angle of  $87.20(14)^\circ$ . The closed triiron core is capped by one S atom. The edge Fe atoms each have three terminal carbonyl groups. Two semibridging carbonyls on the central Fe3 bind the edge Fe4 and Fe5 [Fe3–C11, 1.804(6); Fe4–C11, 2.418(6); Fe3–C12, 1.797(6); Fe5–C12, 2.410(5)  $\text{\AA}$ ]. In particular, the Fe–C<sub>semibridging</sub> bonds of 2.418(6) and 2.410(5)  $\text{\AA}$  are beyond the scope of the Fe–C single bonds [2.0–2.2  $\text{\AA}$ ] and remarkably longer than those of **1** and **2**; this is strongly supported by the

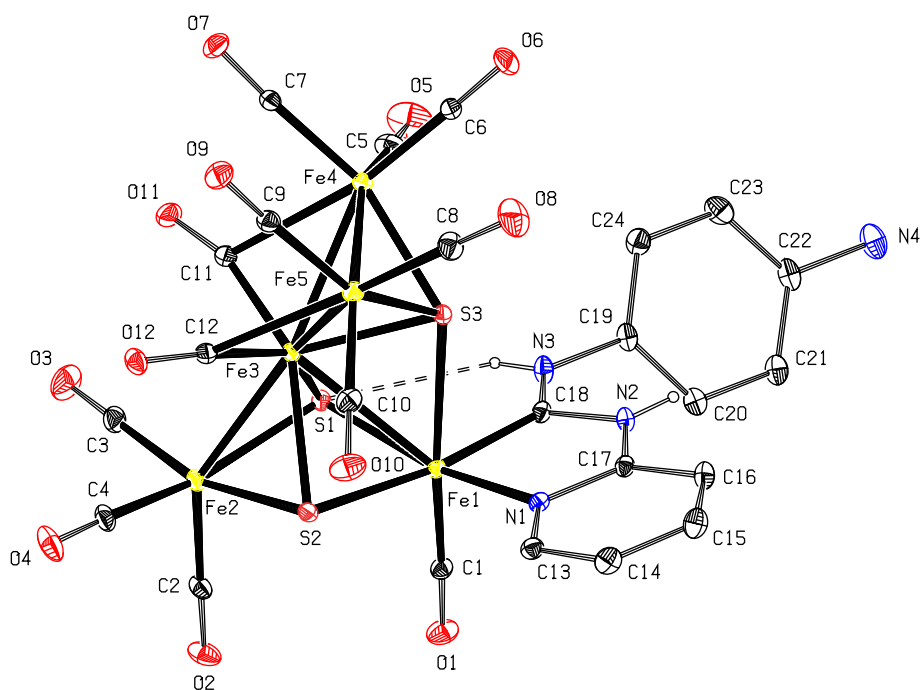


Figure 7. Molecular structure of **13**. Selected geometric parameters ( $\text{\AA}$ ,  $^\circ$ ): Fe1–Fe3, 2.7737(5); Fe2–Fe3, 2.5810(5); Fe3–Fe4, 2.6047(5); Fe3–Fe5, 2.6111(5); Fe4–Fe5, 2.5940(6); Fe1–S1, 2.2141(8); Fe2–S1, 2.2486(8); Fe1–S3, 2.6150(7); Fe1–N1, 2.004(2); Fe1–C18, 1.912(3); Fe3–C11–Fe4, 74.89(10); Fe3–C12–Fe5, 74.26(10); C1–Fe1–S3, 175.31(9).

FT-IR data for **11**. For the reported diiron complex,  $\text{C}_{14}\text{H}_7\text{NFe}_2\text{O}_6$ , the following related values are listed for comparison: IR,  $1881\text{ cm}^{-1}$ ; Fe–C<sub>bridging</sub>, 1.798(5), 2.426(5)  $\text{\AA}$ ; Fe–C–O,  $125.8(4)^\circ$ ,  $163.5(4)^\circ$  [57(b)]. Among the five Fe–Fe bonds, the Fe1–Fe3 bond of 2.7780(10)  $\text{\AA}$  is considerably longer than the others, approaching the high limit of the Fe–Fe single bonds [2.43–2.88] [25(b), 56, 57]. The distance between Fe1 and S3 is 2.5808(15)  $\text{\AA}$ , beyond the normal scope of the Fe–S bonds [2.18–2.37  $\text{\AA}$ ] [3], but closer to the sum of the covalent radii for Fe and S [ $r$ , covalent radius;  $R$ , van der Waals radius;  $r(\text{Fe}) = 1.45$ ,  $r(\text{S}) = 1.04$ ,  $r(\text{Fe}) + r(\text{S}) = 2.49$   $\text{\AA}$ ;  $R(\text{Fe}) = 2.14$ ,  $R(\text{S}) = 1.80$ ,  $R(\text{Fe}) + R(\text{S}) = 3.94$   $\text{\AA}$ ] [51], thereby, the interaction between Fe1 and S3 may be viewed as a weak bond with a C1–Fe1–S3 angle of  $176.6(2)^\circ$  [61].

Cluster **13** (figure 7) also consists of a bent triiron and a closed triiron framework sharing a vertex. The two triangles are not coplanar, the dihedral angle being  $88.48(2)^\circ$ . The open triiron core is capped by two S atoms above and below with an Fe1–Fe3–Fe2 angle of  $78.671(15)^\circ$ . The  $\text{S}_2\text{Fe}_3$  subcore in **13** displays a distorted square-pyramidal geometry. The chelating carbene ligand, through C18 and pyridine N1, is equatorially coordinated to the basal Fe1 with Fe1–C18 = 1.912(3)  $\text{\AA}$  and Fe1–N1 = 2.004(2)  $\text{\AA}$ . The angle sum of C18 [Fe1–C18–N2,  $114.05(18)^\circ$ ; Fe1–C18–N3,  $129.0(2)^\circ$ ; N2–C18–N3,  $116.9(2)^\circ$ ] is  $360.0(2)^\circ$ , showing that C18 is  $\text{sp}^2$ -hybridized. The three irons Fe1–Fe3–Fe2 with the chelating ligand forms a dihedral angle of  $85.89(7)^\circ$ , the  $\text{C}_6\text{H}_4$  plane with the chelating ligand makes a dihedral angle of  $66.38(13)^\circ$ , smaller than the  $79.5(4)^\circ$  angle observed in **12**. The closed triiron



core is capped by one S which is weakly bound to the basal Fe1 with the Fe1–S3 separation of 2.6150(7) Å and C1–Fe1–S3 angle of 175.31(9)°. The edge Fe atoms each have three terminal carbonyl groups. Two semibridging carbonyl groups on the central Fe3 bind the edge Fe4 and Fe5, respectively [Fe3–C11, 1.812(3); Fe4–C11, 2.402(3); Fe3–C12, 1.804(3); Fe5–C12, 2.440(3) Å]. The presence of long Fe–CO<sub>semibridging</sub> bonds is supported by the FT-IR data of **13**.

As shown in figure 8, **14** belongs to the above S<sub>3</sub>Fe<sub>5</sub> type with five Fe–Fe bonds. The two triangles are not coplanar, their dihedral angle being 87.92(3)°. The open triiron core is capped by two S atoms above and below with a triiron angle of 78.16(2)°. As mentioned above, the S<sub>2</sub>Fe<sub>3</sub> subcore in **14** has a distorted square-pyramidal geometry. The chelating carbene is coordinated equatorially to the basal Fe1 with Fe1–C18 = 1.912(4) and Fe1–N1 = 2.005(3) Å. The two C18–N bond lengths are 1.344(5) and 1.338(5) Å [C18–N2 and C18–N3, respectively]. The angle sum [359.9(3)°] of C18 [Fe1–C18–N2, 114.4(3)°; Fe1–C18–N3, 126.8(3)°; N2–C18–N3, 118.7(3)°] is indicative of sp<sup>2</sup>-hybridized C. Due to the Fe–CN<sub>2</sub> unit being coplanar with the C<sub>5</sub>H<sub>4</sub>N ring, these atoms form a larger conjugated system, leading to the short Fe–C<sub>carbene</sub> bond. The chelating ligand is vertical with the open triiron atoms, with a dihedral angle of 89.63(11)°, the uncoordinated C<sub>5</sub>H<sub>4</sub>N ring makes a dihedral angle of 2.6(5)° with the chelating ligand. The closed triiron core is capped by one S which is weakly linked to the basal Fe1 with an Fe1–S3 separation of 2.5762(10) Å and a C1–Fe1–S3 angle of 174.82(13)°. The edge Fe atoms each have three terminal carbonyl groups

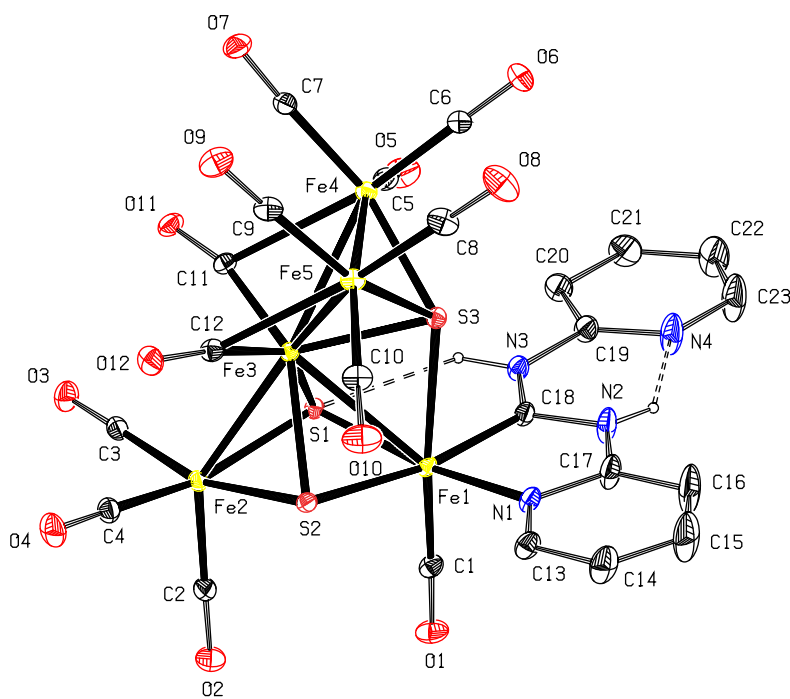


Figure 8. Molecular structure of **14**. Selected geometric parameters (Å,°): Fe1–Fe3, 2.7844(6); Fe2–Fe3, 2.5949(7); Fe3–Fe4, 2.6199(7); Fe3–Fe5, 2.6121(8); Fe4–Fe5, 2.5916(7); Fe1–S1, 2.2113(9); Fe1–S2, 2.2767(9); Fe1–S3, 2.5762(10); Fe1–N1, 2.005(3); Fe1–C18, 1.912(4); Fe1–Fe3–Fe2, 78.16(2); Fe3–C11–Fe4, 73.75(12); Fe3–C12–Fe5, 73.88(13); C1–Fe1–S3, 174.82(13).

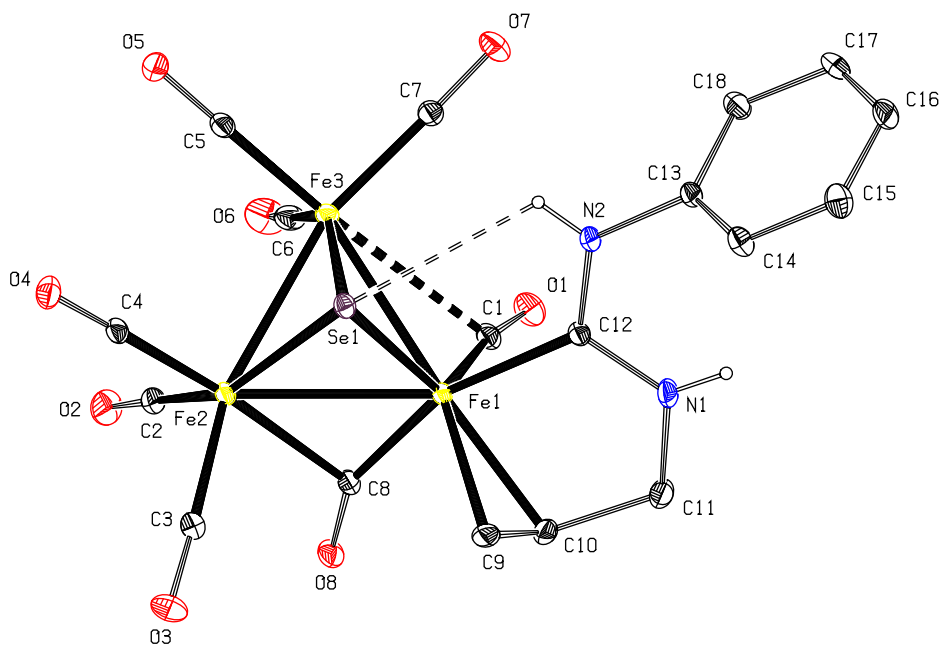


Figure 9. Molecular structure of **16**. Selected geometric parameters ( $\text{\AA}$ , $^\circ$ ): Fe1–Fe2, 2.6714(5); Fe2–Fe3, 2.6015(6); Fe1–Fe3, 2.6391(6); Fe1–Se1, 2.3104(5); Fe2–Se1, 2.3109(5); Fe3–Se1, 2.3321(5); Fe1–C8, 1.844(3); Fe2–C8, 2.217(3); Fe1–C9, 2.113(3); Fe1–C10, 2.121(3); C9–C10, 1.386(4); Fe1–C12, 1.994(2); Fe1–C8–Fe2, 81.70(10); Fe1–C1–O1, 170.9(3).

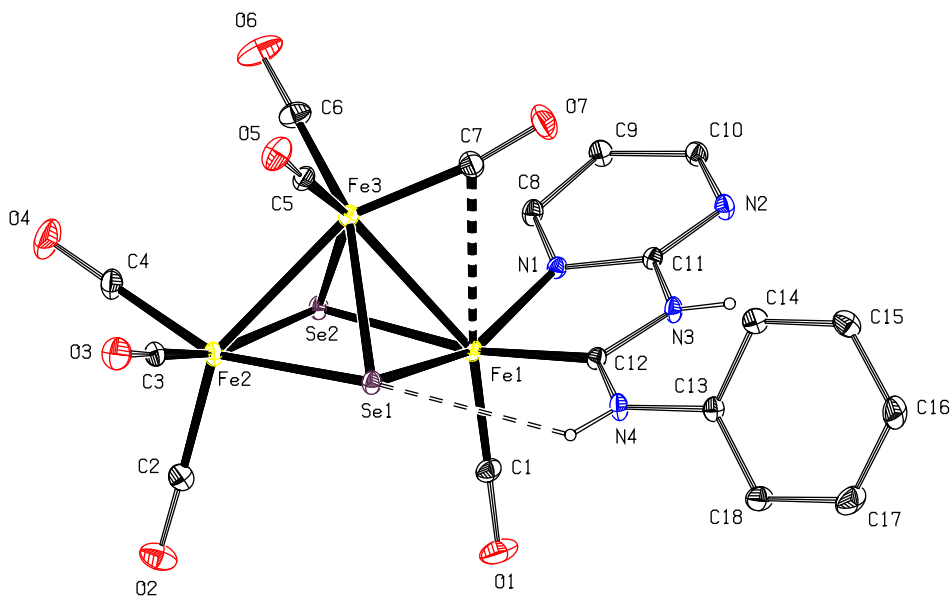


Figure 10. Molecular structure of **17**. Selected geometric parameters ( $\text{\AA}$ , $^\circ$ ): Fe1–N1, 2.007(2); Fe1–Fe3, 2.6632(7); Fe2–Fe3, 2.5976(7); Fe1–Se1, 2.3281(6); Fe2–Se1, 2.3786(6); Fe3–Se1, 2.3997(6); Fe1–Se2, 2.3656(6); Fe2–Se2, 2.3901(6); Fe3–Se2, 2.4040(6); Fe1–C12, 1.913(3); Fe1...C7, 2.757(4); Fe1–Fe3–Fe2, 85.56(2); Fe3–C7–O7, 171.9(4).

groups. Two semibridging carbonyl groups on the central Fe atom Fe3 are bound to the edge Fe4 and Fe5 [Fe3–C11, 1.811(4); Fe4–C11, 2.466(4); Fe3–C12, 1.814(4); Fe5–C12, 2.449(4) Å]; the FT-IR data of **14** confirm the presence of the long Fe–CO<sub>semibridging</sub> bonds.

The known bow-tie clusters with two closed triiron rings are [<sup>n</sup>BuN<sub>4</sub>]<sub>2</sub>[Fe<sub>5</sub>(CO)<sub>14</sub>(μ<sub>3</sub>-S)<sub>2</sub>] [**60(a)**], [(PPh<sub>3</sub>)<sub>2</sub>N]<sub>2</sub>[Fe<sub>5</sub>(CO)<sub>14</sub>(μ<sub>3</sub>-S)<sub>2</sub>] [**60(b)**], [Et<sub>4</sub>N]<sub>3</sub>[HFe<sub>5</sub>(CO)<sub>14</sub>] [**60(c)**], and [Fe<sub>5</sub>(CO)<sub>14</sub>(C<sub>2</sub>R)<sub>2</sub>] (R = Me, Et) [**60(d)**]. Moreover, the ‘parent’ cluster corresponding to **11–15**, S<sub>3</sub>Fe<sub>5</sub>(CO)<sub>14</sub> with 20 skeletal electrons ( $n = 8$ , the Wade-Mingos rules), is still unknown [61]. Therefore, the clusters **11–15** with chelating carbene ligands, (μ<sub>3</sub>-S)<sub>2</sub>(μ<sub>4</sub>-S)Fe<sub>5</sub>(CO)<sub>10</sub>(μ-CO)<sub>2</sub>(κ<sup>2</sup>N,C-L<sub>2</sub>) (L<sub>2</sub> = C<sub>carbene</sub>-N<sub>heterocycle</sub> ligand), are the first example.

Cluster **16** (figure 9) consists of a triangular core of irons with two short Fe–Fe bonds [Fe2–Fe3, 2.6015(6) Å; Fe1–Fe3, 2.6391(6) Å] and one long Fe–Fe bond [Fe1–Fe2, 2.6714(5) Å]. The selenide ligand, which is 1.7469(3) Å away from the triiron plane, almost symmetrically caps the triiron plane. Three terminal carbonyls are on Fe2 and Fe3 and one terminal carbonyl on Fe1 to which the chelating ligand is bonded. The carbonyl on Fe1 semibridges Fe2 [Fe1–C8, 1.844(3) Å; Fe2–C8, 2.217(3) Å; Fe1–C8–O8, 152.9(2)°; Fe2–C8–O8, 125.0(2)°; Fe1–C8–Fe2, 81.70(10)°], the presence of which is supported by the FT-IR data of **16**. The terminal carbonyl on Fe1 is bent toward Fe3, with Fe3...C1 = 2.742(3) Å and Fe1–C1–O1 = 170.9(3)°. As in **1**, the Fe1–C12 bond of 1.994(2) Å in **16** is a typical Fe–C single bond. Similarly, Fe1–C9 and Fe1–C10 bonds of 2.113(3) and 2.121(3) Å are single bonds, whereas the C9–C10 bond of 1.386(4) Å has some double-bond character. The carbene C–N bond lengths are 1.320(3) [C12–N1] and 1.339(3) Å [C12–N2]. The sum of angles about C12 [Fe1–C12–N1, 116.6(2); Fe1–C12–N2, 126.6(2); N1–C12–N2, 116.9(2)°] is 360.1(2)°, indicating that carbene C12 is sp<sup>2</sup>-hybridized. Therefore, these values of the bond lengths and angles show that the C12, N1, and N2 form a conjugated system. In the case of **16**, the carbene C12 acts only as an *n* donor. As in **1**, the chelating carbene ligand functions as a four-electron donor in a κ<sup>3</sup>C<sub>3</sub>C<sub>3</sub> fashion. According to electron-counting rules, each iron conforms to the 18-electron rule. The carbene C12 lies approximately *trans* to one arm of the semibridging carbonyl [C8–Fe1–C12, 160.31(11)°]. The Fe1C9C10 plane forms a dihedral angle of 88.53(18)° with the carbene CN<sub>2</sub> group and the CN<sub>2</sub> group forms a dihedral angle of 71.06(14)° with the phenyl plane. Not surprisingly, as the Se analog of **1**, **16** shows similar geometric parameters.

Cluster **17** (figure 10) has a bent triangle of Fe atoms capped by two Se atoms above and below with a triiron angle of 85.56(2)° and is the Se analog of **9**. The Se<sub>2</sub>Fe<sub>3</sub> core adopts a distorted square-pyramidal geometry analogous to the previously reported cluster (μ<sub>3</sub>-Se)<sub>2</sub>Fe<sub>3</sub>(CO)<sub>9</sub> [59(a), 62]. In (μ<sub>3</sub>-Se)<sub>2</sub>Fe<sub>3</sub>(CO)<sub>9</sub>, each of the two Se atoms on the square base triply bridges the two basal Fe(CO)<sub>3</sub> units on the same base and the third Fe(CO)<sub>3</sub> group at the apex of the pyramid, and each of the three Fe atoms satisfies the 18-electron rule. Thereby, **17** may be formally viewed as involving replacement of the two equatorial carbonyl ligands on one of the iron centers on the square base in (μ<sub>3</sub>-Se)<sub>2</sub>Fe<sub>3</sub>(CO)<sub>9</sub> by a four-electron chelating carbene group, viz. carbene C and pyrimidine N. The carbene ligand causes significant structural effects, an increase in the triiron bond angle compared with (μ<sub>3</sub>-Se)<sub>2</sub>Fe<sub>3</sub>(CO)<sub>9</sub> [83.21(3)°], and an increase in the Fe–Fe bond-length difference from 0.0121(10) to 0.0656(7) Å. The Fe1–Fe3 and Fe2–Fe3 bond lengths are 2.6632(7) and 2.5976(7) Å whereas those lengths in (μ<sub>3</sub>-Se)<sub>2</sub>Fe<sub>3</sub>(CO)<sub>9</sub> are 2.6448(10) and 2.6569(10) Å [59(a)]. The Fe1–N1 bond length is 2.007(2) Å and practically equals those of **6** and **9**. The Fe1–C12 bond length of 1.913(3) Å is equal to that of **7**. The C12–N bond lengths of

1.365(4) and 1.337(4) Å and the angle sum [359.9(2)°] of the carbene C12 [Fe1–C12–N3, 114.0(2)°; Fe1–C12–N4, 129.8(2)°; N3–C12–N4, 116.1(3)°] indicate the  $\pi$ -electron delocalization over the carbene CN<sub>2</sub> group. Because the Fe–CN<sub>2</sub> unit is coplanar with the C<sub>4</sub>H<sub>3</sub>N<sub>2</sub> ring, these atoms form a larger conjugated system resulting in the short Fe–C<sub>carbene</sub> bond. The chelating ligand makes a dihedral angle of 80.27(14) and 60.07(15)° with the open tri-iron plane and the phenyl ring, respectively. The Fe3–Se bond lengths of 2.3997(6) and 2.4040(6) Å in **17** are longer than the other Fe–Se bond lengths [2.3281(6)–2.3901(6) Å]. Notably, one of the three carbonyl ligands attached to the apical Fe3 weakly interacts with the carbene-substituted basal Fe1 from a direction *trans* to C1O1 [Fe1···C7, 2.757(4) Å], leading to nonlinearity of the Fe3–C7–O7 bond angle [Fe3–C7–O7, 171.9(4)°] with carbonyl C7 bent toward Fe1.

Each *N,N'*-disubstituted thiourea can exist in solution as two conformers, resulting from either a *trans* or *cis* orientation of the H–N and C=S bonds with respect to the N–C bond, namely *trans/cis* and *trans/trans* isomers [63], accordingly, the corresponding coordinated carbene generated from cleavage of the CS bond may also show two types of *trans/cis* and *trans/trans* conformations depicted in chart 2, arising from either a *trans* or *cis* orientation of the H–N and Fe–C<sub>carbene</sub> bonds with respect to the N–C<sub>carbene</sub> bond. However, as shown in figures 1–6 and 8–10, each exhibits the first type (I) owing to the stabilized intramolecular hydrogen bonding, viz. *trans/cis*, the second (II) being excluded due to steric repulsion. As described below, it is this conformation that involves the self-assembly of each new cluster.

### 3.3. Packing modes of clusters

Since assembly based on the H–NC<sub>carbene</sub> group as an H-bonding donor and the CO ligand as an H-bonding acceptor as well as the CO dipole–dipole interactions are rare [64], the self-assemblies of the clusters described below should be interesting (see Supplementary Data). Cluster **1** crystallizing in the *P2<sub>1</sub>/c* space group with a KPI of 69.7 via a centrosymmetric dimer generated from a [C16–H16···O5<sup>i</sup>] hydrogen bond forms a [2 0 1] infinite 1-D chain linked by an [N1–H1···O8<sup>ii</sup>] hydrogen bond (figure 1S) (symmetry codes: (i) 1 – x, 1 – y, 1 – z; (ii) –1 + x, 3/2 – y, –1/2 + z; C16···O5<sup>i</sup>, 3.451(3) Å; N1–H1, 0.85(3) Å; H1···O8<sup>ii</sup>, 2.40(3) Å; N1···O8<sup>ii</sup>, 3.192(3) Å; N1–H1···O8<sup>ii</sup>, 155(2)°). Unlike **1**, **2** in the *P1* space group with a KPI of 68.1 exists in the form of a centrosymmetric dimer generated from a [C9–H9B···O3<sup>i</sup>] hydrogen bond (figure 2S) (symmetry code: (i) 1 – x, 1 – y, 1 – z; C9···O3<sup>i</sup>, 3.254(10) Å). Cluster **3** crystallizes in the *P2<sub>1</sub>/c* space group with a KPI of 67.6 and with two different molecules (**3a** and **3b**) in the asymmetric unit. Molecules **3a** and **3b** each form a centrosymmetric dimer generated from [N2–H2···O7<sup>i</sup>] or [N6–H6···O14<sup>ii</sup>] hydrogen bonds (figure 3S) (symmetry codes: (i) 1 – x, 1 – y, 1 – z; (ii) –x, –y, –z; N2–H2, 0.82(3) Å; H2···O7<sup>i</sup>, 2.37(3) Å; N2···O7<sup>i</sup>, 3.138(5) Å; N2–H2···O7<sup>i</sup>, 157(3)°; N6–H6, 0.80(5) Å; H6···O14<sup>ii</sup>, 2.34(5) Å; N6···O14<sup>ii</sup>, 3.073(5) Å; N6–H6···O14<sup>ii</sup>, 152(5)°). There are no directional interactions between the two dimers. Cluster **4** crystallizing in the *I2/a* space group with a KPI of 66.9 exists as a centrosymmetric dimer generated from an [N2–H2···O7<sup>i</sup>] hydrogen bond (figure 4S) (symmetry code: (i) 1/2 – x, 1/2 – y, 1/2 – z; N2···O7<sup>i</sup>, 3.226(4) Å). Unlike **5**, **6** crystallizes in the *P1* space group with a KPI of 69.1. The centrosymmetric dimer is generated from a [C10–H10···O6<sup>i</sup>] hydrogen bond. The dimers are connected to form a [0 1 0] infinite chain by an [N3–H3···O6<sup>ii</sup>] hydrogen bond (figure 5S) (symmetry codes: (i) 1 – x, 1 – y, 1 – z; (ii) x, 1 + y, z;

C10...O6<sup>i</sup>, 3.319(5) Å; N3–H3, 0.82(4) Å; H3...O6<sup>ii</sup>, 2.57(4) Å; N3...O6<sup>ii</sup>, 3.242(5) Å; N3–H3...O6<sup>ii</sup>, 140(4)°. Cluster **7** crystallizes in the  $P2_1/c$  space group with a KPI of 70.6. The molecules form a (1 0 1) sheet via [N2–H2...O5<sup>i</sup>] and [N3–H3B...O1<sup>ii</sup>] hydrogen bonds. These sheets are further packed by an [N3–H3B...O4<sup>iii</sup>] hydrogen bond to lead to an infinite 3-D network (figure 6S) (symmetry codes: (i)  $-1 + x, 1/2 - y, -1/2 + z$ ; (ii)  $x, 1/2 - y, -1/2 + z$ ; (iii)  $1 - x, -1/2 + y, 1/2 - z$ ; N2–H2, 0.84(3) Å; H2...O5<sup>i</sup>, 2.59(3) Å; N2...O5<sup>i</sup>, 3.310(3) Å; N2–H2...O5<sup>i</sup>, 144(3)°; N3–H3B, 0.85(4) Å; H3B...O1<sup>ii</sup>, 2.59(4) Å; N3...O1<sup>ii</sup>, 3.191(4) Å; N3–H3B...O1<sup>ii</sup>, 129(3)°; N3–H3B, 0.85(4) Å; H3B...O4<sup>iii</sup>, 2.54(4) Å; N3...O4<sup>iii</sup>, 3.295(4) Å; N3–H3B...O4<sup>iii</sup>, 148(4)°. Cluster **8** crystallizing in the  $P\bar{1}$  space group with the disordered CH<sub>2</sub>Cl<sub>2</sub> exists as a centrosymmetric dimer generated from an [N2–H2...O1<sup>i</sup>] hydrogen bond (figure 7S) (symmetry code: (i)  $1 - x, 1 - y, 1 - z$ ; N2–H2, 0.88(3) Å; H2...O1<sup>i</sup>, 2.54(4) Å; N2...O1<sup>i</sup>, 3.282(3) Å; N2–H2...O1<sup>i</sup>, 142(3)°). Unlike **8**, **9** crystallizing in the  $P2_1/c$  space group with a KPI of 68.8 forms a [1 0 0] infinite chain (figure 8S) via an [N3–H3...O5<sup>i</sup>] hydrogen bond (plus C4≡O4... $\pi$ (Cg1<sup>i</sup>) and C5≡O5... $\pi$ (Cg2<sup>i</sup>)) (symmetry code: (i)  $-1 + x, y, z$ ; Cg1, centroid of the pyrimidyl ring; Cg2, centroid of the phenyl ring; N3–H3, 0.78(3) Å; H3...O5<sup>i</sup>, 2.54(3) Å; N3...O5<sup>i</sup>, 3.247(3) Å; N3–H3...O5<sup>i</sup>, 153(3)°; O4...Cg1<sup>i</sup>, 3.566(3) Å; O5...Cg2<sup>i</sup>, 3.779(3) Å). Cluster **10** in the  $Pccn$  space group with a KPI of 67.7 via a weak [C11–H11...S2<sup>i</sup>] hydrogen bond forms a [0 0 1] infinite chain (symmetry code: (i)  $3/2 - x, y, 1/2 + z$ ; C11...S2<sup>i</sup>, 3.552(4) Å). The H bonded to N2 is not involved in H-bonding (figure 9S). Cluster **11** in the  $P2_1/c$  space group via a [C16–H16...O9<sup>i</sup>] hydrogen bond forms a [0 0 1] infinite chain. These chains are linked along the *b* axis by a [C25–H25B...O4<sup>ii</sup>] hydrogen bond to lead to a (1 0 0) sheet, viz. 2-D network (figure 10S) (symmetry codes: (i)  $x, 3/2 - y, 1/2 + z$ ; (ii)  $1 - x, 1/2 + y, 1/2 - z$ ; C16...O9<sup>i</sup>, 3.201(7) Å; C25...O4<sup>ii</sup>, 3.13(2) Å). The MeOC<sub>6</sub>H<sub>4</sub> group and CH<sub>2</sub>Cl<sub>2</sub> are disordered; therefore, the packing mode only refers to the main part of **11**. Analogous to **10**, the H bonded to N2 is not involved in H-bonding. Cluster **12** in the  $P2_1/c$  space group with a KPI of 67.8 via a centrosymmetric dimer generated from an [N3–H3...N4<sup>i</sup>] intermolecular hydrogen bond forms a (1 0 0) 2-D network linked by an [N2–H2...O11<sup>ii</sup>] intermolecular hydrogen bond (figure 11S) (symmetry codes: (i)  $1 - x, 1 - y, 1 - z$ ; (ii)  $1 - x, -1/2 + y, 1/2 - z$ ; N3–H3, 0.78(8) Å; H3...N4<sup>i</sup>, 2.36(8) Å; N3...N4<sup>i</sup>, 3.062(9) Å; N3–H3...N4<sup>i</sup>, 150(8)°; N2–H2, 0.89(8) Å; H2...O11<sup>ii</sup>, 2.43(8) Å; N2...O11<sup>ii</sup>, 3.272(10) Å; N2–H2...O11<sup>ii</sup>, 159(7)°). Cluster **13** crystallizes in the  $C2/c$  space group with a KPI of 67.8. The centrosymmetric dimer is generated from a weak [N4–H4A...O2<sup>i</sup>] intermolecular hydrogen bond. The dimers are linked via C1...O2<sup>ii</sup> and O1...C2<sup>ii</sup> interactions to lead to a [1 1 0] double chain (symmetry codes: (i)  $1 - x, 1 - y, 1 - z$ ; (ii)  $1/2 - x, 1/2 - y, 1 - z$ ; N4–H4A, 0.94(4) Å; H4A...O2<sup>i</sup>, 2.60(4) Å; N4...O2<sup>i</sup>, 3.085(4) Å; N4–H4A...O2<sup>i</sup>, 113(3)°; C1...O2<sup>ii</sup>, 3.128(4) Å; O1...C2<sup>ii</sup>, 3.128(4) Å). As can be seen in figure 12S, because of being shielded by carbonyls in the dimer, the N4–H4B and N2–H2 groups do not engage in hydrogen bonding. Cluster **14** in the  $P2_1/c$  space group with a KPI of 65.4 forms a dimer via a [C16–H16...O6<sup>i</sup>] intermolecular hydrogen bond. These dimers are linked by an O5...S2<sup>ii</sup> contact to produce a [0 1 0] double chain (figure 13S) (symmetry codes: (i)  $-1 + x, -1 + y, -1 + z$ ; (ii)  $-x, -1/2 + y, 1/2 - z$ ; C16...O6<sup>i</sup>, 3.397(6) Å; O5...S2<sup>ii</sup>, 3.20(1) Å). As shown in figure 13S, the HNCNH unit only takes part in intramolecular hydrogen bonds. Cluster **15** crystallizes in the  $P2_1/c$  space group with a KPI of 64.8, with two different molecules (**15a** and **15b**) in the asymmetric unit. Molecule **15a** forms a chain in the *c* direction via an [N3–H3...O10<sup>i</sup>] hydrogen bond and these chains are linked, along the *b* axis, via [C16–H16...O11<sup>ii</sup>], [N2–H2...O12<sup>ii</sup>], and [C19–H19A...O12<sup>ii</sup>] hydrogen bonds to lead to an *A* sheet. Molecule **15b** forms a [0 1 0]

chain via [N5–H5···O23<sup>iii</sup>], [C37–H37···O24<sup>iii</sup>], and [C40–H40B···O23<sup>iii</sup>] hydrogen bonds and these chains are linked, along the *c* axis, by an [N6–H6···O22<sup>iv</sup>] hydrogen bond to produce an *A* sheet (figure 14S) (symmetry codes: (i)  $x, 1/2 - y, -1/2 + z$ ; (ii)  $-x, 1/2 + y, 3/2 - z$ ; (iii)  $1 - x, -1/2 + y, 3/2 - z$ ; (iv)  $1 - x, 1 - y, 1 - z$ ; N3···O10<sup>i</sup>, 3.30(2) Å; C16···O11<sup>ii</sup>, 3.398(16) Å; N2···O12<sup>ii</sup>, 3.563(14) Å; N5···O23<sup>iii</sup>, 3.491(12) Å; C40···O23<sup>iii</sup>, 3.394(16) Å; N6···O22<sup>iv</sup>, 3.172(13) Å). Directional interactions between the sheets are not observed. Cluster **16** shows a packing mode similar to **1**. Cluster **16** in the  $P2_1/n$  space group with a KPI of 69.9 occurs as a centrosymmetric dimer generated from a [C16–H16···O5<sup>i</sup>] hydrogen bond and forms a [10 $\bar{1}$ ] infinite double chain linked by an [N1–H1···O8<sup>ii</sup>] hydrogen bond (symmetry codes: (i)  $1 - x, 1 - y, 1 - z$ ; (ii)  $-1/2 + x, 1/2 - y, 1/2 + z$ ; C16···O5<sup>i</sup>, 3.450(4) Å; N1–H1, 0.79(3) Å; H1···O8<sup>ii</sup>, 2.47(3) Å; N1···O8<sup>ii</sup>, 3.232(3) Å; N1–H1···O8<sup>ii</sup>, 162(3)°). As shown in figure 15S, an [N2–H2···Se1] intramolecular H-bond is observed. Cluster **17** crystallizes in the  $P2_1/c$  space group with a KPI of 69.0. The molecules form a 1-D chain along the *a*-axis direction via an [N3–H3···O5<sup>i</sup>] hydrogen bond. By an [O2···O6<sup>ii</sup>] contact, these 1-D chains are packed in the *c*-axis direction to result in (1 0 1) 2-D sheets. As shown in figure 16S, an [N4–H4···Se1] intramolecular H-bond is observed (symmetry codes: (i)  $1 + x, y, z$ ; (ii)  $x, 3/2 - y, -1/2 + z$ ; N3–H3, 0.81(3) Å; H3···O5<sup>i</sup>, 2.54(3) Å; N3···O5<sup>i</sup>, 3.219(4) Å; N3–H3···O5<sup>i</sup>, 141(3)°; O2···O6<sup>ii</sup>, 2.893 Å). Cluster **18** in the  $P2_12_12_1$  space group (ignoring the disordered H<sub>2</sub>O) gives a [1 0 0] chain via a [C8–H8···O8<sup>i</sup>] hydrogen bond (symmetry code: (i)  $-1/2 + x, 1/2 - y, 1 - z$ ; C8···O8<sup>i</sup>, 3.446(4) Å). As in **11**, the H attached to N2 does not participate in intermolecular hydrogen bonding (figure 17S). According to the above description, indeed, these new organometallic clusters display an interesting supramolecular-structure spectrum.

#### 4. Conclusion

Eighteen SF<sub>2</sub>, S<sub>2</sub>Fe<sub>3</sub>, S<sub>3</sub>Fe<sub>5</sub>, SeFe<sub>3</sub>, and Se<sub>2</sub>Fe<sub>3</sub> clusters with chelating diaminocarbenes have been synthesized by reactions of substituted thioureas and selenoureas with iron carbonyls and structurally characterized by X-ray crystallography. By virtue of N–H···N, N–H···O, and C–H···O intermolecular hydrogen bonds and other non-covalent interactions, these organometallic clusters display interesting supramolecular structures from 0-D (dimers or tetramers) to 1-D chains, 2-D sheets, or 3-D networks. The reactions of other thioureas, selenoureas and related thioamides and selenoamides with iron carbonyls are under investigation.

#### Supplementary material

CCDC 1043067-1043086 contain the supplementary crystallographic data (including structure factors) for this article. These data can be obtained free of charge from the Cambridge Crystallographic Data Center via [www.ccdc.cam.ac.uk/data\\_request/cif](http://www.ccdc.cam.ac.uk/data_request/cif).

#### Disclosure statement

The authors declare no competing financial interest.

## Funding

The authors are grateful to the Mao Zedong Foundation of China, Project Funded by the Priority Academic Program Development of Jiangsu Higher Education Institutions (PAPD), Natural Science Foundation of China [grant number 20572091], and Natural Science Foundation of Jiangsu Province [grant number 05KJB150151] for financial support of this work.

## Supplementary data

Supplementary data related to this article can be accessed online at <http://dx.doi.org/10.1080/00958972.2015.1079312>.

## References

- [1] (a) L.-C. Song. *Acc. Chem. Res.*, **38**, 21 (2005); (b) L.-C. Song. *Sci. Chin. Ser. B-Chem.*, **52**, 1 (2009).
- [2] H. Ogino, S. Inomata, H. Tobita. *Chem. Rev.*, **98**, 2093 (1998).
- [3] M. Shieh, C.-Y. Miu, Y.-Y. Chu, C.-N. Lin. *Coord. Chem. Rev.*, **256**, 637 (2012).
- [4] S.C. Lee, W. Lo, R.H. Holm. *Chem. Rev.*, **114**, 3579 (2014).
- [5] T. Spatzal, K.A. Perez, O. Einsle, J.B. Howard, D.C. Rees. *Science*, **345**, 1620 (2014).
- [6] G.A.N. Felton, C.A. Mebi, B.J. Petro, A.K. Vannucci, D.H. Evans, R.S. Glass, D.L. Lichtenberger. *J. Organomet. Chem.*, **694**, 2681 (2009).
- [7] W. Lubitz, H. Ogata, O. Rüdiger, E. Reijerse. *Chem. Rev.*, **114**, 4081 (2014).
- [8] (a) T.R. Simmons, G. Berggren, M. Bacchi, M. Fontecave, V. Artero. *Coord. Chem. Rev.*, **270–271**, 127 (2014); (b) T. Xu, D. Chen, X. Hu. *Coord. Chem. Rev.*, **303**, 32 (2015).
- [9] (a) X. Zhao, Y.-M. Hsiao, C.-H. Lai, J.H. Reibenspies, M.Y. Darensbourg. *Inorg. Chem.*, **41**, 699 (2002); (b) X. Zhao, I.P. Georgakaki, M.L. Miller, R. Mejia-Rodriguez, C.-Y. Chiang, M.Y. Darensbourg. *Inorg. Chem.*, **41**, 3917 (2002); (c) M.B. Sárosi, R.B. King, I. Silaghi-Dumitrescu. *Inorg. Chim. Acta*, **363**, 3575 (2010); (d) D. Seyferth, R.S. Henderson, L.-C. Song. *Organometallics*, **1**, 125 (1982); (e) D. Seyferth, G.B. Womack, M.K. Gallagher, M. Cowie, B.W. Hames, J.P. Fackler Jr, A.M. Mazany. *Organometallics*, **6**, 283 (1987).
- [10] (a) Y.-C. Shi, H. Tan, Y. Shi. *Polyhedron*, **67**, 218 (2014); (b) W. Hieber, P. Spacu. *Z. Anorg. Allg. Chem.*, **233**, 353 (1937); (c) J.A. De Beer, R.J. Haines. *J. Organomet. Chem.*, **24**, 757 (1970); (d) L.-C. Song, C.-H. Qi, H.-L. Bao, X.-N. Fang, H.-B. Song. *Organometallics*, **31**, 5358 (2012); (e) X.-F. Liu, Z.-Q. Jiang, Z.-J. Jia. *Polyhedron*, **33**, 166 (2012); (f) P.-H. Zhao, K.-K. Xiong, W.-J. Liang, E.-J. Hao. *J. Coord. Chem.*, **68**, 968 (2015); (g) C.-G. Li, Y. Zhu, F. Xue, M.-J. Cui, J.-Y. Shang. *J. Coord. Chem.*, **68**, 2361 (2015).
- [11] W.-F. Liaw, C. Kim, M.Y. Darensbourg, A.L. Rheingold. *J. Am. Chem. Soc.*, **111**, 3591 (1989).
- [12] (a) W.-F. Liaw, J.-H. Lee, H.-B. Gau, C.-H. Chen, G.-H. Lee. *Inorg. Chim. Acta*, **322**, 99 (2001); (b) Y. Ohki, K. Yasumura, K. Kuge, S. Tanino, M. Ando, Z. Li, K. Tatsumi. *Proc. Nat. Acad. Sci. USA*, **105**, 7652 (2008); (c) L.D. Rosenheim, P.E. Fanwick. *J. Organomet. Chem.*, **431**, 327 (1992); (d) N.M. Zusuzsa. *Bull. Soc. Chim. Belg.*, **100**, 445 (1991).
- [13] (a) J. Takács, L. Markó. *J. Organomet. Chem.*, **247**, 223 (1983); (b) A. Winter, L. Zsolnai, G. Huttner. *Chem. Ber.*, **115**, 1286 (1982); (c) A. Winter, L. Zsolnai, G. Huttner. *J. Organomet. Chem.*, **250**, 409 (1983).
- [14] (a) D. Seyferth, G.B. Womack, J.C. Dewan. *Organometallics*, **4**, 398 (1985); (b) D. Seyferth, G.B. Womack, C.M. Archer, J.C. Dewan. *Organometallics*, **8**, 430 (1989); (c) D. Seyferth, G.B. Womack, C.M. Archer, J.P. Fackler Jr, D.O. Marler. *Organometallics*, **8**, 443 (1989); (d) L.-C. Song, L. Li, Y.-Y. Hu, H.-B. Song. *J. Organomet. Chem.*, **743**, 123 (2013); (e) L.-C. Song, H. Tan, A.-G. Zhu, Y.-Y. Hu, H. Chen. *Organometallics*, **34**, 1730 (2015).
- [15] R.B. King, P.M. Treichel, F.G.A. Stone. *J. Am. Chem. Soc.*, **83**, 3600 (1961).
- [16] D. Seyferth, J.B. Hoke. *Organometallics*, **7**, 524 (1988).
- [17] (a) A.E. Ogilvy, M. Draganjac, T.B. Rauchfuss, S.R. Wilson. *Organometallics*, **7**, 1171 (1988); (b) K. Kobayashi, M. Hirotsu, I. Kinoshita. *Organometallics*, **32**, 5030 (2013).
- [18] (a) A. Shaver, P.J. Fitzpatrick, K. Steliou, I.S. Butler. *J. Am. Chem. Soc.*, **101**, 1313 (1979); (b) J. Windhager, U.-P. Apfel, T. Yoshino, N. Nakata, H. Görls, M. Rudolph, A. Ishii, W. Weigand. *Chem. Asian J.*, **5**, 1600 (2010).
- [19] (a) H.G. Raubenheimer, L. Linford, A.V.A. Lombard. *Organometallics*, **8**, 2062 (1989); (b) C. Alvarez-Toledano, J. Enriquez, R.A. Toscano, M. Martínez-García, E. Cortés-Cortés, Y.M. Osornio, O. García-Mellado, R. Gutiérrez-Pérez. *J. Organomet. Chem.*, **577**, 38 (1999); (c) M.C. Ortega-Alfaro, J.G. López-Cortés, R.A. Toscano, C. Alvarez-Toledano. *J. Braz. Chem. Soc.*, **16**, 362 (2005); (d) M.C. Ortega-Alfaro, O. Alcantara, M. Orrala, J.G. López-Cortés, R.A. Toscano, C. Alvarez-Toledano. *Organometallics*, **26**, 1895 (2007).

- [20] (a) A.Q. Daraosheh, H. Görls, M. El-khateeb, G. Mloston, W. Weigand. *Eur. J. Inorg. Chem.*, **2011**, 349 (2011); (b) H. Alper, A.S.K. Chan. *J. Am. Chem. Soc.*, **95**, 4905 (1973).
- [21] (a) H. Alper, C.K. Foo. *Inorg. Chem.*, **14**, 2928 (1975); (b) H. Alper, A.S.K. Chan. *J. Chem. Soc., Chem. Commun.*, 724 (1973).
- [22] H. Alper, A.S.K. Chan. *Inorg. Chem.*, **13**, 225 (1974).
- [23] H. Alper, D.A. Brandes. *Organometallics*, **10**, 2457 (1991).
- [24] A. Benoit, J.-Y. Le Marouille, C. Mahé, H. Patin. *J. Organomet. Chem.*, **218**, C67 (1981).
- [25] (a) Y.-C. Shi, H.-R. Cheng, Q. Fu, F. Gu, Y.-H. Wu. *Polyhedron*, **56**, 160 (2013); (b) Y.-C. Shi, H.-R. Cheng, H. Tan. *J. Organomet. Chem.*, **716**, 39 (2012); (c) Y.-C. Shi, F. Gu. *Chem. Commun.*, **49**, 2255 (2013).
- [26] (a) H. Patin, G. Mignani, A. Benoit, J.-Y. Le Marouille, D. Grandjean. *Inorg. Chem.*, **20**, 4351 (1981); (b) H. Patin, G. Mignani, R. Dabard, A. Benoit. *J. Organomet. Chem.*, **168**, C21 (1979); (c) H. Patin, G. Mignani, C. Mahé, J.-Y. Le Marouille, T.G. Southern, A. Benoit, D. Grandjean. *J. Organomet. Chem.*, **197**, 315 (1980); (d) D. Seyferth, G.B. Womack, M. Cowie, B.W. Hames. *Organometallics*, **3**, 1891 (1984); (e) A. Lagadec, B. Misterkiewicz, A. Darchen, D. Grandjean, A. Mousser, H. Patin. *Organometallics*, **7**, 242 (1988); (f) B. Dadamoussa, A. Darchen, P. L'Haridon, C. Larpent, H. Patin, J.-Y. Thepot. *Organometallics*, **8**, 564 (1989).
- [27] T. Murai. In *Organoselenium Chemistry*, T. Wirth (Ed.), Chap. 6, pp. 257–281, Wiley-VCH Verlag GmbH & Co. KGaA, Weinheim (2012).
- [28] (a) Y.-C. Shi, Q. Fu. *Z. Anorg. Allg. Chem.*, **639**, 1791 (2013); (b) Y.-C. Shi, H.-R. Cheng, D.-C. Cheng. *Acta Crystallogr. C*, **69**, 581 (2013); (c) W. Yang, Q. Fu, J. Zhao, H.-R. Cheng, Y.-C. Shi. *Acta Crystallogr. C*, **70**, 528 (2014); (d) Y.-C. Shi, Y. Shi, W. Yang. *J. Organomet. Chem.*, **772–773**, 131 (2014); (e) Y.-C. Shi, W. Yang, Y. Shi, D.-C. Cheng. *J. Coord. Chem.*, **67**, 2330 (2014); (f) Y. Shi, Y.-C. Shi. *J. Coord. Chem.*, **68**, 2633 (2015); (g) Y.-C. Shi, Y. Shi, J.-P. Li, Q. Tan, W. Yang, S. Xie. *J. Coord. Chem.*, **68**, 2620 (2015); (h) Y.-C. Shi, Y. Shi. *Inorg. Chim. Acta*, **434**, 92 (2015).
- [29] R. Siebenlist, H.-W. Frühauf, K. Vrieze, H. Kooijman, W.J.J. Smeets, A.L. Spek. *Organometallics*, **19**, 3016 (2000).
- [30] R.B. King. *Organometallic Syntheses: Transition Metal Compounds*, Academic Press, New York, NY, Vol. 1, p. 95 (1965).
- [31] F.-Q. He, X.-H. Liu, B.-L. Wang, Y.-H. Li, Z.-M. Li. *Chin. J. Chem.*, **26**, 1481 (2008).
- [32] G. L'abbé. *Synthesis*, **1987**, 525 (1987).
- [33] A.Z. Muresan, P. Thamyonkit, J.R. Diers, D. Holten, J.S. Lindsey, D.F. Bocian. *J. Org. Chem.*, **73**, 6947 (2008).
- [34] Ó. López, S. Maza, V. Ulgar, I. Maya, J.G. Fernández-Bolaños. *Tetrahedron*, **65**, 2556 (2009).
- [35] K. Ramadas, N. Srinivasan, N. Janarthanan. *Tetrahedron Lett.*, **34**, 6447 (1993).
- [36] K. Ganapati. *J. Indian Chem. Soc.*, **15**, 525 (1938).
- [37] A.K. Mishra, S.B. Mishra, N. Manav, R. Kumar, Sharad, R. Chandra, D. Saluja, N.K. Kaushik. *Spectrochim. Acta, Part A*, **66**, 1042 (2007).
- [38] G. Li, D.-J. Che, Z.-F. Li, Y. Zhu, D.-P. Zou. *New J. Chem.*, **26**, 1629 (2002).
- [39] K. Kamala, P.J. Rao, K.K. Reddy. *Synth. Commun.*, **19**, 2621 (1989).
- [40] A. Gupta, P. Mishra, S.N. Pandeya, S.K. Kashaw, V. Kashaw, J.P. Stables. *Eur. J. Med. Chem.*, **44**, 1100 (2009).
- [41] S. Kubota, K. Horie, H.K. Misra, K. Toyooka, M. Uda, M. Shibuya, H. Terada. *Chem. Pharm. Bull.*, **33**, 662 (1985).
- [42] A. Saxena, R.D. Pike. *J. Chem. Crystallogr.*, **37**, 755 (2007).
- [43] J. Valdés-Martínez, S. Hernández-Ortega, D.X. West, L.J. Ackerman, J.K. Swearingen, A.K. Hermetet. *J. Mol. Struct.*, **478**, 219 (1999).
- [44] M. Koketsu, H. Ishihara. *Curr. Org. Synth.*, **3**, 439 (2006).
- [45] (a) Y.-T. Fan, H.-J. Lu, H.-W. Hou, Z.-M. Zhou, Q.-H. Zhao, L.-P. Zhang, F.-H. Cheng. *J. Coord. Chem.*, **50**, 65 (2000); (b) M.B. Ferrari, F. Bisceglie, E. Cavalli, G. Pelosi, P. Tarasconi, V. Verdolino. *Inorg. Chim. Acta*, **360**, 3233 (2007).
- [46] S.S. Kandil, S.M.A. Katib, N.H.M. Yarkandi. *Transition Met. Chem.*, **32**, 791 (2007).
- [47] M. Koketsu, T. Kiyokuni, T. Sakai, H. Ando, H. Ishihara. *Chem. Lett.*, **35**, 626 (2006).
- [48] M.C. Burla, R. Caliendo, M. Camalli, B. Carrozzini, G.L. Cascarano, C. Giacobozzo, M. Mallamo, A. Mazzone, G. Polidori, R. Spagna. *J. Appl. Crystallogr.*, **45**, 357 (2012).
- [49] G.M. Sheldrick. *Acta Crystallogr. A*, **64**, 112 (2008).
- [50] L.J. Farrugia. *J. Appl. Crystallogr.*, **45**, 849 (2012).
- [51] A.L. Spek. *Acta Crystallogr. D*, **65**, 148 (2009).
- [52] C.F. Macrae, P.R. Edgington, P. McCabe, E. Pidcock, G.P. Shields, R. Taylor, M. Towler, J. van de Streek. *J. Appl. Crystallogr.*, **39**, 453 (2006).
- [53] (a) K. Riener, S. Haslinger, A. Raba, M.P. Högerl, M. Cokoja, W.A. Herrmann, F.E. Kühn. *Chem. Rev.*, **114**, 5215 (2014); (b) J. Vignolle, X. Cattoën, D. Bourissou. *Chem. Rev.*, **109**, 3333 (2009); (c) K. Öfele, E. Tosh, C. Taubmann, W.A. Herrmann. *Chem. Rev.*, **109**, 3408 (2009); (d) P. de Frémont, N. Marion, S.P. Nolan. *Coord. Chem. Rev.*, **253**, 862 (2009); (e) S. Diez-González, N. Marion, S.P. Nolan. *Chem. Rev.*, **109**, 3612



- (2009); (f) D. Bourissou, O. Guerret, F.P. Gabbaï, G. Bertrand. *Chem. Rev.*, **100**, 39 (2000); (g) R.D. Adams. *Chem. Rev.*, **89**, 1703 (1989).
- [54] (a) L. Markó, T. Madach, H. Vahrenkamp. *J. Organomet. Chem.*, **190**, C67 (1980); (b) G. Hogarth, N.J. Taylor, A.J. Carty, A. Meyer. *J. Chem. Soc., Chem. Commun.*, 834 (1988).
- [55] (a) A.V. Virovets, S.N. Konchenko, D. Fenske. *J. Struct. Chem.*, **43**, 694 (2002); (b) D. Belletti, C. Graiff, C. Massera, A. Minarelli, G. Predieri, A. Tiripicchio, D. Acquotti. *Inorg. Chem.*, **42**, 8509 (2003).
- [56] (a) R.K. Hocking, T.W. Hambley. *Organometallics*, **26**, 2815 (2007); (b) S.E. Harris, A.G. Orpen, I.J. Bruno, R. Taylor. *J. Chem. Inf. Model.*, **45**, 1727 (2005).
- [57] (a) B. Zhu, Y. Chen, W. Shi, Y. Li, X. Hao. *Organometallics*, **31**, 4046 (2012); (b) K. Badyal, W.R. McWhinnie, T.A. Hamor, H. Chen. *Organometallics*, **16**, 3194 (1997); (c) R.K. Brown, J.M. Williams, A.J. Schultz, G.D. Stucky, S.D. Ittel, R.L. Harlow. *J. Am. Chem. Soc.*, **102**, 981 (1980).
- [58] (a) G. Huttner, W. Gartzke. *Chem. Ber.*, **105**, 2714 (1972); (b) S. Warratz, L. Postigo, B. Royo. *Organometallics*, **32**, 893 (2013); (c) I. Yu, C.J. Wallis, B.O. Patrick, P.L. Diaconescu, P. Mehrhodavandi. *Organometallics*, **29**, 6065 (2010).
- [59] (a) R. Seidel, B. Schnautz, G. Henkel. *Angew. Chem. Int. Ed.*, **35**, 1710 (1996); (b) C.H. Wei, L.F. Dahl. *Inorg. Chem.*, **4**, 493 (1965); (c) W.-S. Hong, C.-Y. Wu, C.-S. Lee, W.-S. Hwang, M.-Y. Chiang. *J. Organomet. Chem.*, **689**, 277 (2004); (d) G. Dettlaf, P. Hübener, J. Klimes, E. Weiss. *J. Organomet. Chem.*, **229**, 63 (1982); (e) A. Benoit, J.-Y. Le Marouille, C. Mahé, H. Patin. *J. Organomet. Chem.*, **233**, C51 (1982); (f) B. Liu, B.-F. Wu, X. Hu, S.-T. Liu, Q.-W. Liu, Z.-R. Zhao. *Acta Chim. Sin.*, **56**, 930 (1998); (g) W. Yang, Q. Fu, J. Zhao, H.-R. Cheng, Y.-C. Shi. *Acta Crystallogr.C*, **70**, 528 (2014).
- [60] (a) R.L. Holliday, L.C. Roof, B. Hargus, D.M. Smith, P.T. Wood, W.T. Pennington, J.W. Kolis. *Inorg. Chem.*, **34**, 4392 (1995); (b) F. Calderoni, F. Demartin, M.C. Iapalucci, F. Laschi, G. Longoni, P. Zanello. *Inorg. Chem.*, **35**, 898 (1996); (c) C. Femoni, M.C. Iapalucci, G. Longoni, S. Zacchini. *Dalton Trans.*, **40**, 8685 (2011); (d) S. Brait, G. Gervasio, D. Marabello, E. Sappa. *J. Chem. Soc., Dalton Trans.*, 989 (2000).
- [61] (a) M.E. O'Neill, K. Wade. *Inorg. Chem.*, **21**, 461 (1982); (b) D.M.P. Mingos. *Acc. Chem. Res.*, **17**, 311 (1984); (c) R.B. King, I. Silaghi-Dumitrescu, A. Kun. *J. Chem. Soc., Dalton Trans.*, 3999 (2002).
- [62] (a) L.F. Dahl, P.W. Sutton. *Inorg. Chem.*, **2**, 1067 (1963); (b) D. Cauzzi, C. Graiff, M. Lanfranchi, G. Predieri, A. Tiripicchio. *J. Organomet. Chem.*, **536–537**, 497 (1997).
- [63] R. Custelcean. *Chem. Commun.*, 295 (2008).
- [64] R. Dubey, M.S. Pavan, T.N.G. Row, G.R. Desiraju. *IUCrJ*, **1**, 8 (2014).